

22
1-10-84 85 ①

I-12754

DE-2018-4

UCID-19948

Flow Visualizations, Velocity Measurements,
and Surface Convection Measurements in
Simulated 20.8-cm Nova Box Amplifier Cavities

Howard L. Julien
Edward L. Molishever

DISCLAIMER

This report was prepared as an account of work sponsored by an agency of the United States Government. Neither the United States Government nor any agency thereof, nor any of their employees, makes any warranty, express or implied, or assumes any legal liability, or responsibility for the accuracy, completeness, or usefulness of any information, apparatus, product, or process disclosed, or represents that its use would not infringe privately owned rights. Reference herein to any specific commercial product, process, or service by trade name, trademark, manufacturer, or otherwise does not necessarily constitute or imply its endorsement, recommendation, or favoring by the United States Government or any agency thereof. The views and opinions of authors expressed herein do not necessarily state or reflect those of the United States Government or any agency thereof.

October 31, 1983

MASTER

Lawrence
Livermore
Laboratory

This is an informal report intended primarily for internal or limited external distribution. The opinions and conclusions stated are those of the author and may or may not be those of the Laboratory.

Work performed under the auspices of the U.S. Department of Energy by the Lawrence Livermore Laboratory under Contract W-7405-Eng-48.

DISTRIBUTION OF THIS DOCUMENT IS UNLIMITED

Interdepartmental letterhead

Mail Station L. 461

Ext: 2-5908

UCID--19948

DE84 004354

October 31, 1983

Nova File - 210


TO: W. W. Simmons

FROM: H. L. Julien/E. L. Molishever

SUBJECT: FLOW VISUALIZATIONS, VELOCITY MEASUREMENTS, AND SURFACE
CONVECTION MEASUREMENTS IN SIMULATED 20.8-CM NOVA BOX AMPLIFIER
CAVITIES

ABSTRACT

Reported are fluid mechanics experiments performed in models of the 20.8-cm Nova amplifier lamp and disk cavities. Lamp cavity nitrogen flows are shown, by both flow visualization and velocity measurements, to be acceptably uniform and parallel to the flashlamps. In contrast, the nitrogen flows in the disk cavity are shown to be disordered. Even though disk cavity flows are disordered, the simplest of three proposed nitrogen introduction systems for the disk cavity was found to be acceptable based on convection measurements made at the surfaces of simulated laser disks.


H. L. Julien


E. L. Molishever

0155F/dj
University of California

 Lawrence Livermore
National Laboratory

NOTICE

PORTIONS OF THIS REPORT ARE ILLEGIBLE.

It has been reproduced from the best available copy to permit the broadest possible availability.

1.0 INTRODUCTION

1.1 BACKGROUND

The relative importance of internal conduction, surface convection and radiant energy exchange during convective cooling of glass laser disks was examined analytically in 1980.^{(1)*} The results obtained suggest rapid cooling of the amplifier lamp cavity and the achievement of uniform convection at the disk surface can significantly reduce the cooling period required between successive laser "shots." The establishment of proper *convective flow patterns inside the amplifier is especially important* in achieving both of these conditions.

Subsequent calculations of amplifier cooling rates for the Nova chain⁽²⁾ indicate 80 percent of the nitrogen gas should be supplied to the larger Nova box amplifiers to achieve uniform cooling of the laser chain components. For assumed constant convective heat transfer coefficients in the lamp cavities and disk cavities, the selected design flows in these amplifiers are:

<u>Amplifier</u>	<u>Lamp Cavities (Total)</u>	<u>Disk Cavity</u>
20.8 cm	12 cfm	18 cfm
31.5 cm	60 cfm	33 cfm
46.0 cm	206 cfm	110 cfm

The corresponding total nitrogen flow for the laser chain is 500 cfm, which results in a cooling period of approximately four hours. However, longer cooling periods are anticipated if the assumed convective conditions do not exist.

The need for proper convective flow patterns in both the lamp cavities and disk cavities became an important criteria in the design of the Nova box amplifiers. The flow studies reported in this memorandum were conducted to verify amplifier designs and to guide the selection of nitrogen introduction systems.

*Numbers in parentheses refer to references listed at the end of this memorandum.

1.2 SCOPE OF THE STUDY

The experiments were intended to provide design information only, in contrast to a definitive study of convection in a laser amplifier. Experimental models were restricted to the size of the 20.8-cm amplifier and nitrogen flow rates were fixed at those adopted for this amplifier size. It was felt that qualitative results obtained can be extrapolated to the 31.5-cm amplifier of similar design. The 46.0-cm amplifier has a somewhat different lamp cavity but the design of this component can be guided by these experiments as well.

1.3 PURPOSE OF THE STUDY

Separate experimental studies of lamp cavity flows and disk cavity flows were conducted to indirectly evaluate convective cooling of the Nova box amplifiers. Flow visualization and velocity measurements were conducted in a transparent model of the 20.8-cm amplifier lamp cavity to:

- o Verify nitrogen flows in the cavity are uniform using a proposed nitrogen introduction system.
- o Obtain an empirical basis for sizing new plenums at each end of the cavity if found necessary.

Flow visualizations and disk surface convection measurements were conducted in a transparent model of the 20.8-cm amplifier disk cavity to:

- o Obtain an understanding of the anticipated three-dimensional flow pattern in the cavity.
- o Investigate the resulting variation of the convective heat transfer coefficient on the disk surfaces.

Three proposed methods of introducing nitrogen into the disk cavity through instrastage hardware were considered in these experiments.

1.4 ORGANIZATION OF THE REPORT

The experiments and the results obtained are summarized in Section 2.0. Test apparatuses for the lamp cavity and disk cavity studies are described in Section 3.0. Experimental techniques and attending data reduction methods are described in Section 4.0. Finally, the experimental results are discussed in detail in Section 5.0.

2.0 SUMMARY AND CONCLUSIONS

Clear plexiglass models of the 20.8-cm box amplifier lamp and disk cavities were fabricated. Flow visualization experiments, using neutrally buoyant bubbles, were performed in the lamp cavity model and attending velocity profiles were measured using hot wire anemometry. In addition to flow visualizations, the spatial distributions of the convective heat transfer coefficient on laser disk surfaces were obtained in the disk cavity model.

2.1 LAMP CAVITY EXPERIMENTS

2.1.1 The Apparatus

A lamp cavity model was fabricated from actual flashlamps, a reflector, and both intake and exhaust gas plenums by mounting them in a clear plexiglass housing designed for this purpose. Air was supplied to the model through the intake plenum and exhausted to the atmosphere through the exhaust plenum.

2.1.2 Flow Visualization

A bubble generator was inserted between the air supply and the lamp cavity model and high-speed photographs of bubble streaks in the cavity were taken. The streaks from each photograph were then superimposed on one tracing of the lamp cavity and the composite picture was analyzed. Conclusions reached were:

1. The flow is apparently uniformly and parallel over the flashlamps
2. Velocity measurement can easily be interpreted and used to establish the degree of flow uniformly in the cavity.

2.1.3 Velocity Measurements

Hot wire anemometer measurements were made in the spaces between flashlamps at three depths and three axial locations. Based on the flow visualization results and these measurements, it was concluded that the flow is uniformly distributed over the flashlamps except near the center of the cavity just downstream of the inlet plenum. However, this non-uniformity near the inlet plenum is limited in extent and, therefore, the plenum design investigated is considered acceptable.

2.2 DISK CAVITY EXPERIMENTS

2.2.1 The Apparatus

A disk cavity model was fabricated from clear plexiglass disks, mounted in a clear plexiglass housing designed for this purpose. Intrastage hardware was simulated with rolled aluminum cylinders and the upstream cylinder contained vanes whose orientation to the flow could be varied. Air was supplied to the model through four ports in this upstream cylinder and exhausted to the atmosphere through a conical diffuser added to the downstream cylinder.

2.2.2 Flow Visualization

A bubble generator was inserted in the upstream cylinder and high-speed photographs of the bubble streaks in the cavity were taken. However, no conclusions could be drawn, except that velocities are low and the flow is disordered.

2.2.3 Disk Surface Measurements

A "China Clay" technique was used to determine evaporation rates at laser disk surfaces for different entrance flow geometries. Spatial distributions of the convective heat transfer coefficient were deduced from the measurements. Conclusions reached were:

1. Turning vanes in the gas introduction system are not necessary if gas is introduced through diametrically-opposed ports in the intrastage hardware.
2. All disk surfaces cool at the same average rate, even though local rates of cooling are different.

2.4 RECOMMENDATIONS

1. The present design of the 20.8-cm amplifier lamp cavity will assure uniform cooling of the flashlamps.
2. Turning vanes need not be used in the disk cavity flow introduction system. Enhanced convective heat transfer through swirling the gas was observed in these tests as initially conceived, but at the expense of nonuniform cooling of the disk surfaces.
3. The designs of the 34.5-cm and 46-cm amplifier gas systems should be guided by these results which must necessarily apply in these larger geometries.

3.0 TEST APPARATUS

Separate transparent models of the 20.8-cm amplifier lamp cavity and disk cavity were used. Descriptions of each model include:

- Construction details
- General physical arrangement in the flow simulation
- Instrumentation
- Qualification tests.

3.1 LAMP CAVITY TEST MODEL

Figures 3.1 thru 3.3 are sketches of the lamp cavity model. Figures 3.1 and 3.2 are isometric front and rear views and Figure 3.3 is a cross-sectional view showing the orientation of the gas induction and exhaust systems relative to the plasma lamps contained in the cavity.

Utilized are actual plasma lamps, actual sheetmetal gas distribution plenums and a reflector similar to the actual 20.8-cm amplifier reflector. The housing is made of welded aluminum and clear plexiglass viewing windows on the front and rear. The windows are bolted into place and have rubber gaskets for sealing. The model is leak-proof, even though there is leakage between the lamp and disk cavities in an actual amplifier.

The reflector was painted black, the plasma lamps green, and the plenums red in order to highlight bubbles used to trace streaklines.

3.1.2 General Physical Arrangement

The lamp cavity housing was connected by plastic tubing to an air supply that entered through the rear of the cavity. Velocity measurements and observations were made from the front of the model.

Two ports supplied air to the inlet plenum, then the air moved along the flashlamps cavity and passed into an identical exhaust plenum.

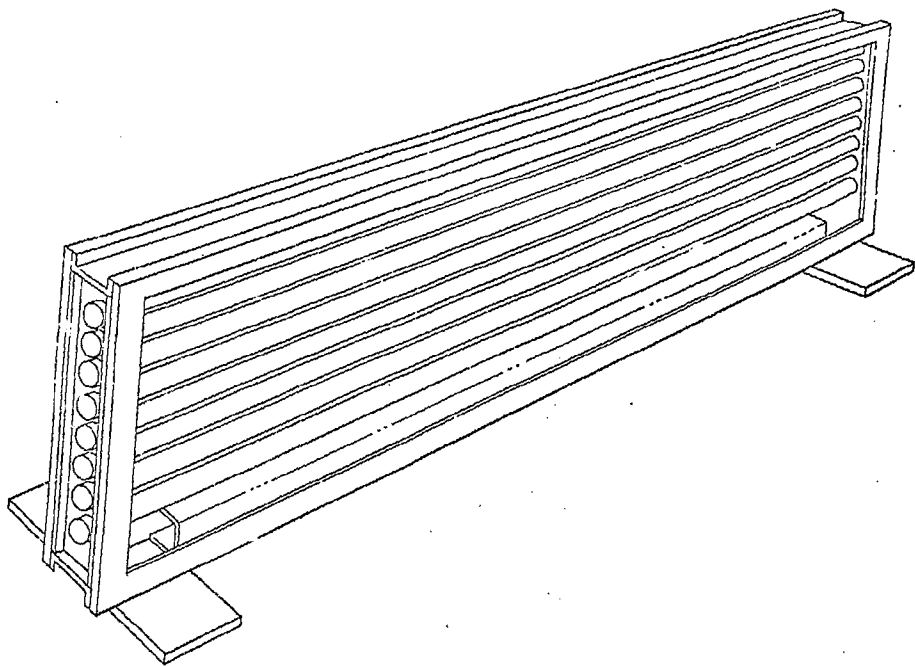


Figure 3.1. Lamp Cavity Test Fixture (Front View).

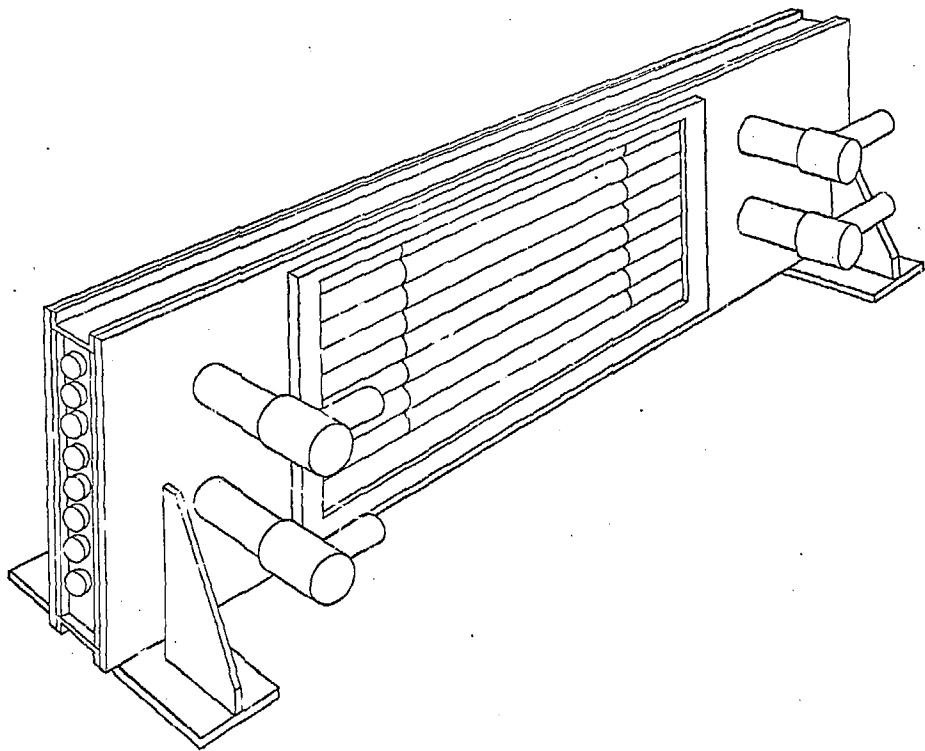


Figure 3.2. Lamp Cavity Test Fixture (Rear View).

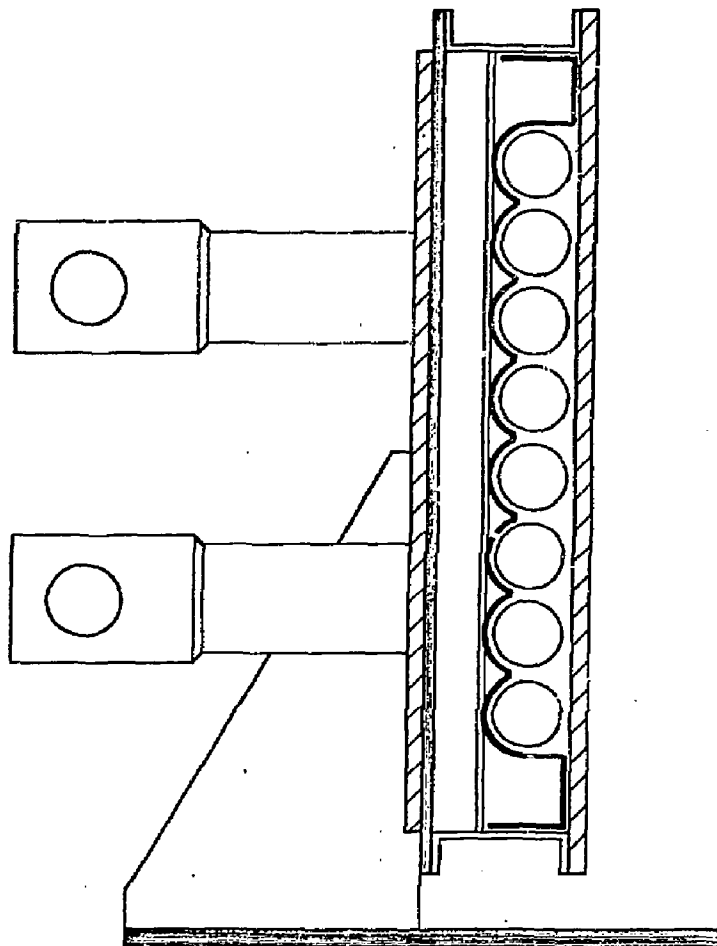


Figure 3.3. Lamp Cavity Test Fixture (Cross Section).

The air then left the exhaust plenum through two ports and exhausted into the laboratory. An orifice meter upstream of the cavity measured the flow which was regulated by a needle valve.

The front face of the cavity can be sealed by one of two different clear plexiglass sheets. One plexiglass sheet was perforated with three columns of holes - seven holes in each column - that can accommodate a temperature compensated hot wire anemometer to measure velocity at different depths. The other plexiglass sheet was unperforated to optimize flow visualization when a bubble generator was inserted in the airline upstream of the lamp cavity to facilitate tracing of fluid streaklines in the cavity.

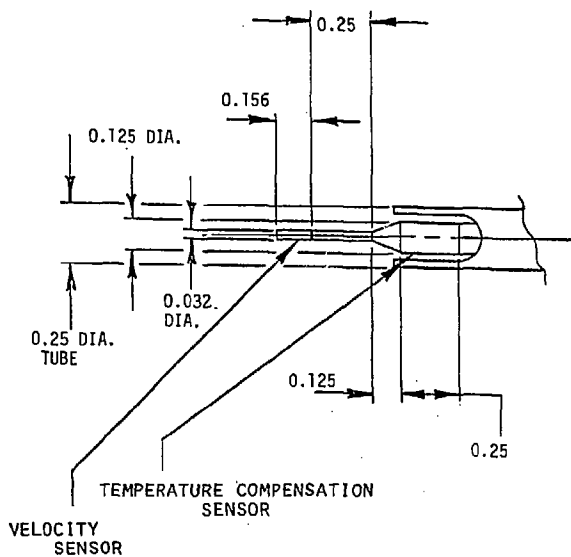
3.1.3 Instrumentation

3.1.3.1 Hot Wire Anemometer

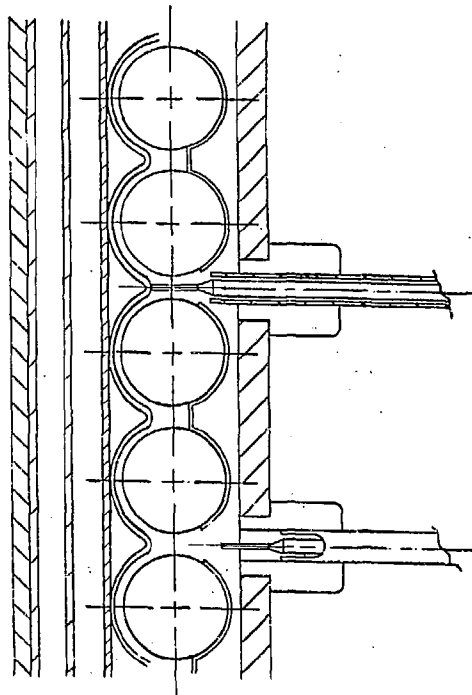
The hot wire anemometer penetrated the perforated face of the lamp cavity as shown in Figure 3.4. Measurements were made with a KURTZ model no. 430-1-4 temperature compensated probe. When new, the probe has a guard around its sensor; however, the guard was removed to permit insertion of the probe between flashlamps. Power was supplied to the probe by a 12-volt D.C. supply and output was measured with a D.C. voltmeter (5 volts full-scale deflection). Velocity was deduced from the calibration chart supplied by KURTZ. The probe was supported by a plastic annulus at each insertion point which kept it perpendicular to the lamp axis. Depth of insertion was determined by scribed marks on the probe.

3.1.3.2 Bubble Generator System

Flow visualization was accomplished with a Sage Action bubble generator. The bubble generating probe (Figure 3.5) was connected to three lines: (1) soap solution, (2) helium, and (3) the air supplied to the test model. The helium interacted with the soap forming bubbles of varying densities which were moved to a vortex separator by the air. The vortex separator eliminated bubbles which were not neutrally buoyant,



DETAIL OF PROBE END -
KURZ AIR VELOCITY SYSTEM 430-DC-2



VELOCITY PROBE PLACEMENT
IN LAMP CAVITY TEST FIXTURE

Figure 3.4. Details of Lamp Cavity Velocity Measurements

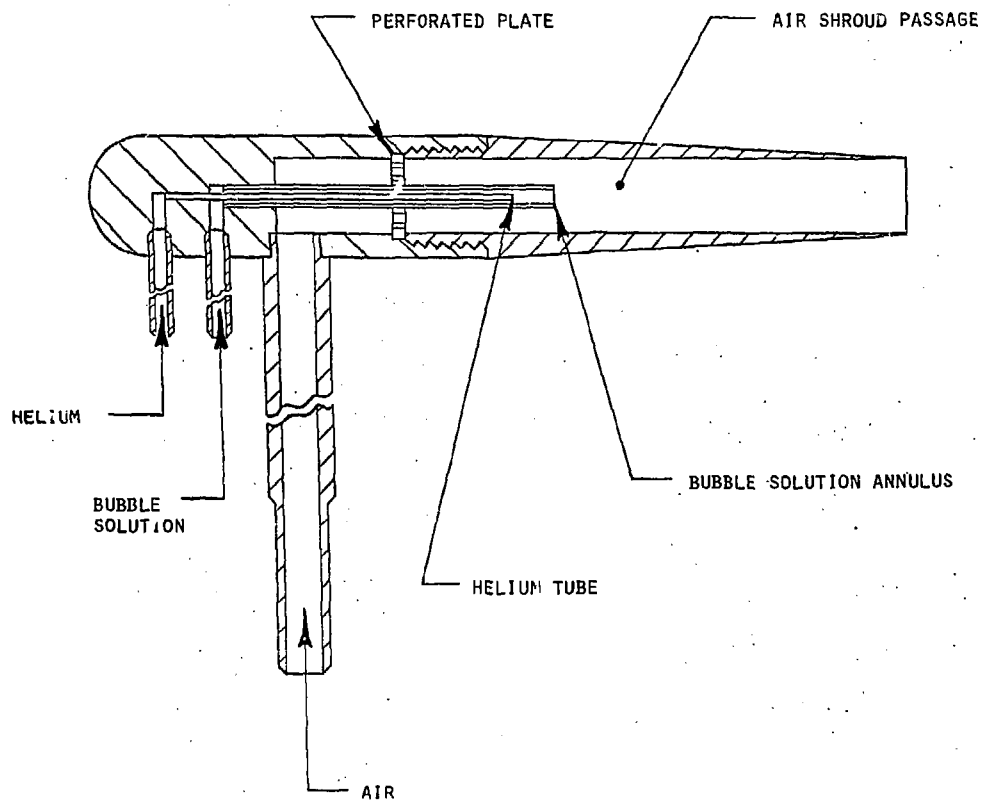


Figure 3.5. Details of Bubble Generation Probe.

The vortex separator is a cylindrical jar with an inlet port for the air in its lateral surface and an outlet port at the top. The tangential entry of the air gave the air a circular motion so that bubbles heavier than air struck the lateral surface of the jar and burst. Bubbles lighter than air spiraled towards the center of the jar where they struck a hollow cylindrical tube which led to the outlet port. Like the heavier bubbles they also burst. Those bubbles which were neutrally buoyant followed streamlines of air and emerged from the outlet port at the center of the top face of the vortex separator. The bubbles and air were then carried to the inlet ports of the lamp cavity.

The bubble field of view was illuminated with a stroboscope whose frequency and flash duration were controlled. Bubble trajectories, therefore, appeared as discontinuous streaks of light when streak length is proportional to bubble velocity. Photographs were made with a fast acting polaroid camera and high speed film.

Bubble trajectories were also recorded on videotape.

3.1.4 Qualification of the Apparatus

Leakage was not permitted from the lamp cavity model since its magnitude could not be predicted and would have been a source of error. The lamp cavity was leak tested by using liquid soap as a leak detector. All leaks were eliminated by sequential checks, bolt tightening and external taping.

Strobe speed, distance from the lamp cavity and the angle of its line of sight with respect to the lamp cavity axis were varied so that clarity of bubble trajectories was optimized and the effect of parallax was minimized. Camera exposure time, focal length and position were also varied to optimize the clarity of bubble trajectories.

The velocity profiles were integrated across the lamp cavity flow cross-section and the resulting total flow was compared to that given by the flow meter. Although velocity measurements were not sufficiently detailed to have an accurate check, no gross error was observed.

Finally, the influence of bubble generating physics on the trajectories was checked by varying the ratios of soap, helium and air. The effect on bubble trajectory was found to be negligible if the vortex generator was used.

3.2 DISK CAVITY MODEL

3.2.1 Disk Cavity Test Model

The 20.8-cm disk cavity was duplicated using clear plexiglass for the cavity and for the three laser disks. Cylindrical plenums upstream and downstream of the disk cavity made of rolled aluminum, simulated the interstage hardware to be used with Nova laser chain. The plexiglass cavity was bolted together and sealed with rubber gaskets. The disks were bolted to aluminum holders which were bolted to the cavity base. Figure 3.6 is an isometric sketch of the model.

3.2.2 General Physical Arrangement

As just mentioned, there were plenums (rolled aluminum cylinders) both upstream and downstream of the disk cavity which simulated the interstage hardware. Figure 3.7 is a sketch of the upstream plenum, that contains turning vanes of variable orientation for swirling the flow. Swirling, it was hoped, would minimize boundary layer development on the leading surface of the upstream disk resulting in a uniform and enhanced convective heat transfer coefficient. Air was introduced to the disk cavity through four ports equally spaced around the lateral surface of the upstream plenum. A base flow case was established by removing the inner liner and, thereby, circumventing the vaned flow channel.

Since the interstage hardware was still being designed, we wished to minimize the effect of flow geometry in the downstream plenum on the flow in the disk cavity model. This was accomplished by putting a flow straightening screen in the plenum and a conical diffuser downstream of the plenum.

Unfiltered air entered the upstream plenum through flexible plastic

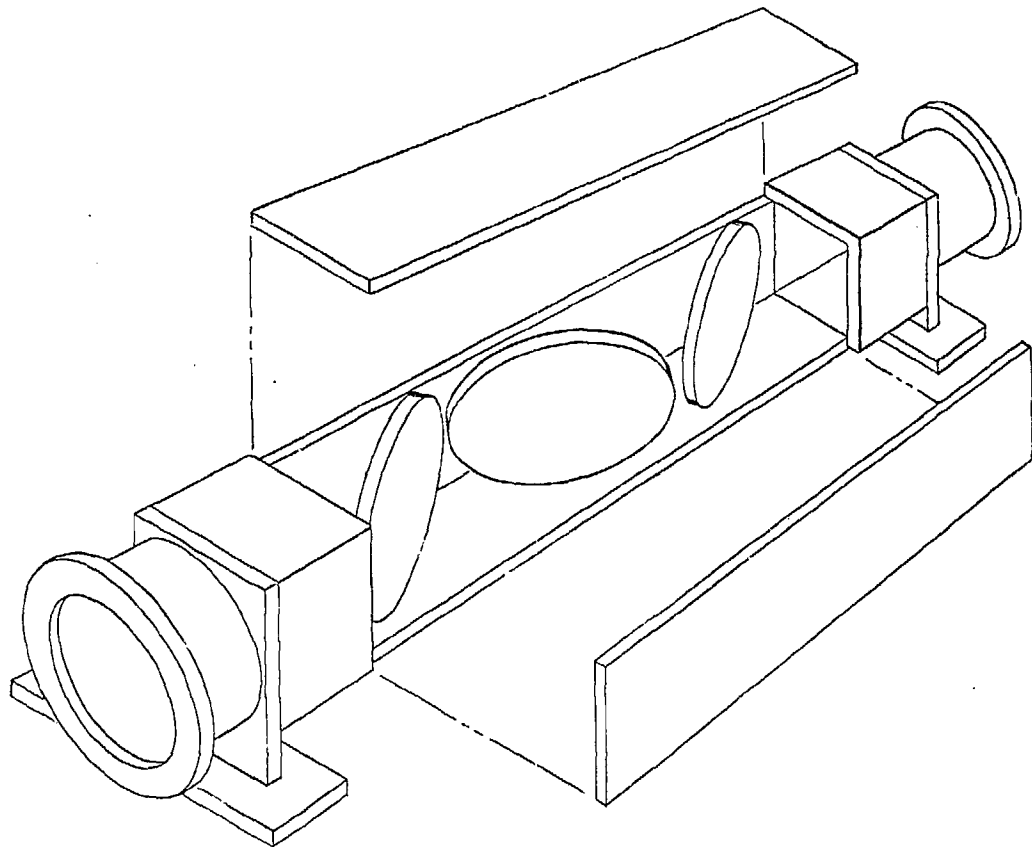


Figure 3.6. Disk Cavity Test Fixture Without Intrastage Hardware

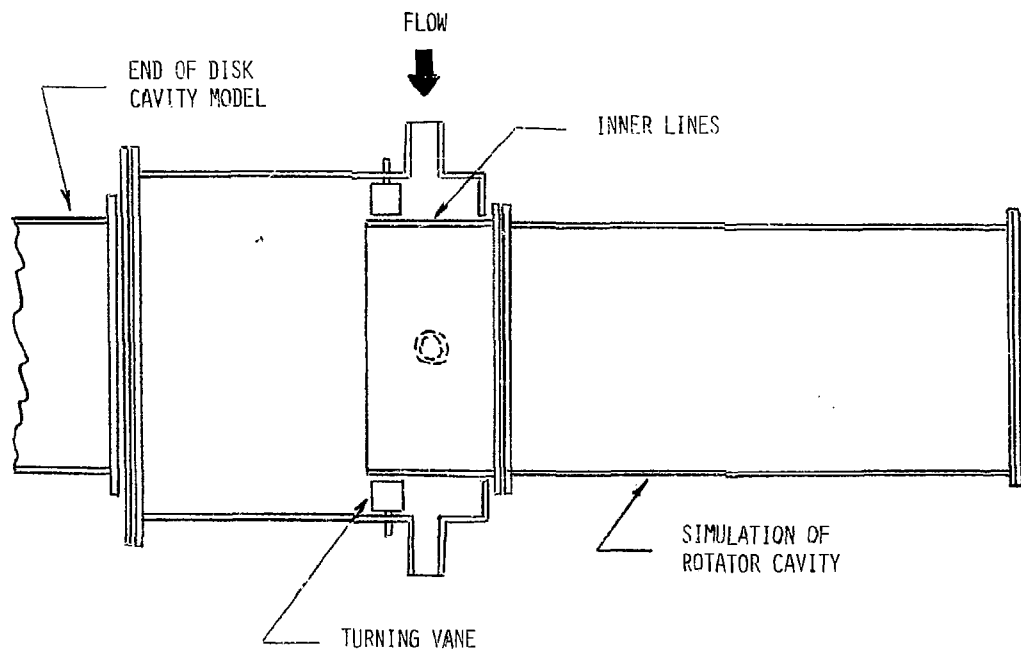


Figure 3.7. Upstream Intrastage Hardware Simulation Using Turning Vanes

tubing and exhausted from the conical diffuser to atmosphere through plastic tubing. Total flowrate was measured with an orifice plate upstream of the disk cavity model and the flow was controlled with a needle valve, also upstream of the cavity.

3.2.3 Instrumentation

As previously mentioned, total flow through the disk cavity was measured with a calibrated orifice plate. Upstream pressure was also measured with a pressure gauge.

A "China Clay" technique was used to determine relative convective heat transfer rates on the surface of the laser disks. First, each clear plastic laser disk surface was coated with "China Clay" which made the surface opaque when it dried. Then, the disk surface to be observed was sprayed with oil of wintergreen which made it transparent. As air flowed over the disk, the oil of wintergreen dried and the disk surface became opaque in the dried regions.

The drying pattern was observed by illuminating the surface with a high intensity lamp. Contrast was improved by placing a black curtain behind the disk cavity. At recorded time intervals, the surface of the disk cavity was videotaped and these records were later used to establish drying rates on the disk surface. These drying rates relate directly to convective heat transfer rates for the investigated flow condition.

Prior to the drying tests, flow visualization tests were conducted using the Sage Action bubble generator discussed in 3.1.3.

3.2.4 Qualification of the Apparatus

The model was leak tested using liquid soap as a leak detector. Initial leaks were eliminated using the procedure outlined for the lamp cavity model.

Test repeatability was checked by repeating the drying test on the surface of the lead disk; test results were nearly identical in duplicate test runs. The vertical orientation of the disk surfaces assured only a thin layer of oil could be supported on the surface and, thusly, aided in achieving this test repeatability.

4.0 EXPERIMENTAL TECHNIQUES AND DATA REDUCTION METHODS

Three different experimental techniques were applied. A description of each technique, how it was applied, the difficulties associated with the application of each technique, and the limitations of each technique are discussed below. The experimental techniques are:

- o Flow visualization using neutrally buoyant bubbles,
- o Hot wire anemometry to determine velocity profiles and,
- o The "China Clay" technique for determining relative convective heat transfer coefficients on laser disk surfaces.

Data reduction methods used are also discussed.

4.1 FLOW VISUALIZATION

4.1.1 Setting the Flow Conditions

Analytical studies had been performed to determine those lamp and disk cavity flow rates in each amplifier which would minimize the cooling time of an amplifier chain. For the 20.8-cm amplifier, optimum flow rates were 6 cfm in each lamp cavity and 18 cfm in the disk cavity. Flow rates to each amplifier cavity were maintained at these levels using a calibrated orifice for measurement.

4.1.2 Flow Visualization Using the Bubble Generator

Flow visualization using bubbles presented challenges both in data taking and in data presentation. At established flows, the bubbles were moving too fast to be tracked by eye. In addition, bubble generation times were erratic and bubble burst probabilities prior to reaching the lamp and disk cavities were high. It was, therefore, hard to capture multiple bubble streaks in the cavities on a single frame of film or video tape. The methods used to minimize these problems and the degree of success achieved were different for the lamp cavity and disk cavity tests.

4.1.2.1 Lamp Cavity Tests

One of the keys to success with this test series was to obtain neutrally buoyant bubbles. At operating flows, the bubbles moved through the lamp cavity too quickly to be observed directly. Therefore, the bubble generator was calibrated at lower flows where the bubbles could be seen by eye.

The bubble generator had three controls: (1) helium flowrate, (2) soap solution flowrate, and (3) air flowrate. Adjustments were made to the bubble generator by adjusting these flow rates. After the initial calibration at low flow, the air flow rate was increased and the flow was photographed.

The frequency and duration of the strobe flashes and the camera exposure time were critical factors in recording streaklines because it was easy to produce underexposed and overexposed photographs with the polaroid camera. The optimum combination of strobe and camera parameters was obtained only after much trial-and-error testing.

Fifteen photographs of bubbles traversing the lamp cavity of acceptable quality were obtained. Appendix A contains reproductions of the photographs and a composite sketch of the observed streaklines is presented as Figure 5.1 in the discussion of results.

4.1.2.2 Disk Cavity Experiments

Bubbles were used for flow visualization at the lead disk in the disk cavity. However, the usefulness of these data is limited by the complexity of the flow pattern. Appendix A contains reproductions of the photographs taken with the bubble generator probe placed inside the inlet plenum of the disk cavity.

4.2 HOT-WIRE TRAVERSING PROCEDURE

Velocity profiles in the lamp cavity were obtained using hot wire anemometry. Compared to the other measurements, the hot-wire measurements were straight forward. The guard on the sensor was first removed so the sensor could pass between flashlamps. The probe was supported by an annulus at each measurement point so the probe traverse was perpendicular to the lamp axis (see Figure 3.4). Scribe marks on the probe made it easy to take measurements at three different depths. It took about a minute for the probe temperature to reach steady-state and the output voltage to be recorded.

4.3 APPLICATION OF THE "CHINA CLAY" TECHNIQUE

4.3.1 Technique to Laser Disk Surfaces.

The "China Clay" technique was used to determine relative convective heat transfer rates at laser disk surfaces. The test procedure consisted of first coating all disk surfaces with kaopectate, which contains China Clay, and, when dried, leaves an opaque surface. Oil of wintergreen was then sprayed over one surface to make it transparent. As air flowed over the disk, opaque patches slowly formed and grew with time. The condition of the surface was videotaped at regular intervals of time and these data were used to establish drying rates on the disk surface.

Lighting and the tone of the background were the key variables which determined the contrast between dried and undried portions of the disk. Both artificial light and sunlight were used and a black curtain was placed behind the amplifier cavity to enhance contrast.

4.4 DATA REDUCTION METHODS

4.4.1 Photographic Documentation of Streakline Patterns

Fifteen photographs were made of streaklines in the lamp cavity

model. As mentioned previously, bubble production was erratic; therefore, no one photograph can define the streaklines in the entire lamp cavity. If, however, the streaklines from all photographs are superimposed onto one diagram of the lamp cavity, a composite figure is developed. This figure was constructed using the photographs taken. All photographs were taken with the camera in the same position with respect to the lamp cavity; consequently, the outline of the lamp cavity and lamps was transferred to a sheet of tracing paper and, then, the streaklines from each photograph were transferred to the tracing paper.

The same procedure could not be followed in the disk cavity tests since the data are sparse.

4.4.2 Reduction of Hot Wire Measurements

The hot wire data were recorded at 63 points (three axial locations, each with seven points between the tubes and at three depths).

The data from the KURTZ hot wire probes were recorded in volts and converted to velocity using a KURTZ supplied calibration curve.

4.4.3 Reduction of Measured Laser Disk Evaporation Rates and Calculation of Equivalent Convective Heat Transfer Coefficients h^*

As previously mentioned, evaporation data were videotaped. The data were subsequently transferred from the video tapes to layouts of the laser disks. This was done by sketching the boundaries of the dried regions and identifying them with the evaporation time. The convective heat transfer rate at each point was determined based on the fact that it is inversely proportional to the evaporation time due to the similarity of heat and mass transfer. The constant of proportionality was obtained by comparing the evaporation data on the lead disk to the variation of the convective heat transfer coefficient along a finite inclined plate, as measured by Sparrow et.al.⁽³⁾.

The comparison is shown in Figure 4.1, where measured evaporation rates on the first disk for the baseline case are graphically matched on the major axis of the elliptical disk to the flat plate correlations.

The correlation used to obtain this match is

$$h^* = 3.0 / \Delta \tau_{\text{EVAP}} \quad (\text{J hr}^{-1} \text{cm}^{-2} \text{C}^{-1}) \quad (4.1)$$

where $\Delta \tau_{\text{EVAP}}$ is the evaporation time in hours.

All evaporation data were reduced with this correlation.

4.4.4 Uncertainty Analysis

Possible errors in the measurements and observations made in this series of tests were considered.

4.4.4.1 Flow Visualization

The fifteen photographs of the lamp cavity with bubble streaks are all similar. This suggests that the data are repeatable. However, there is a gradual upward trend of the bubble streaklines both on the photographs and the superimposed picture. The uniformity of the velocity profiles at the downstream axial position implies that the upward trend is the result of bubble buoyancy rather than a physical occurrence at the exhaust plenum.

4.4.4.2 Hot Wire Measurements

The manufacturer of the hot wire anemometer rates his device as accurate to within $\pm 2\%$ of the actual velocity. The measured velocity profiles should be reliable to this level of accuracy.

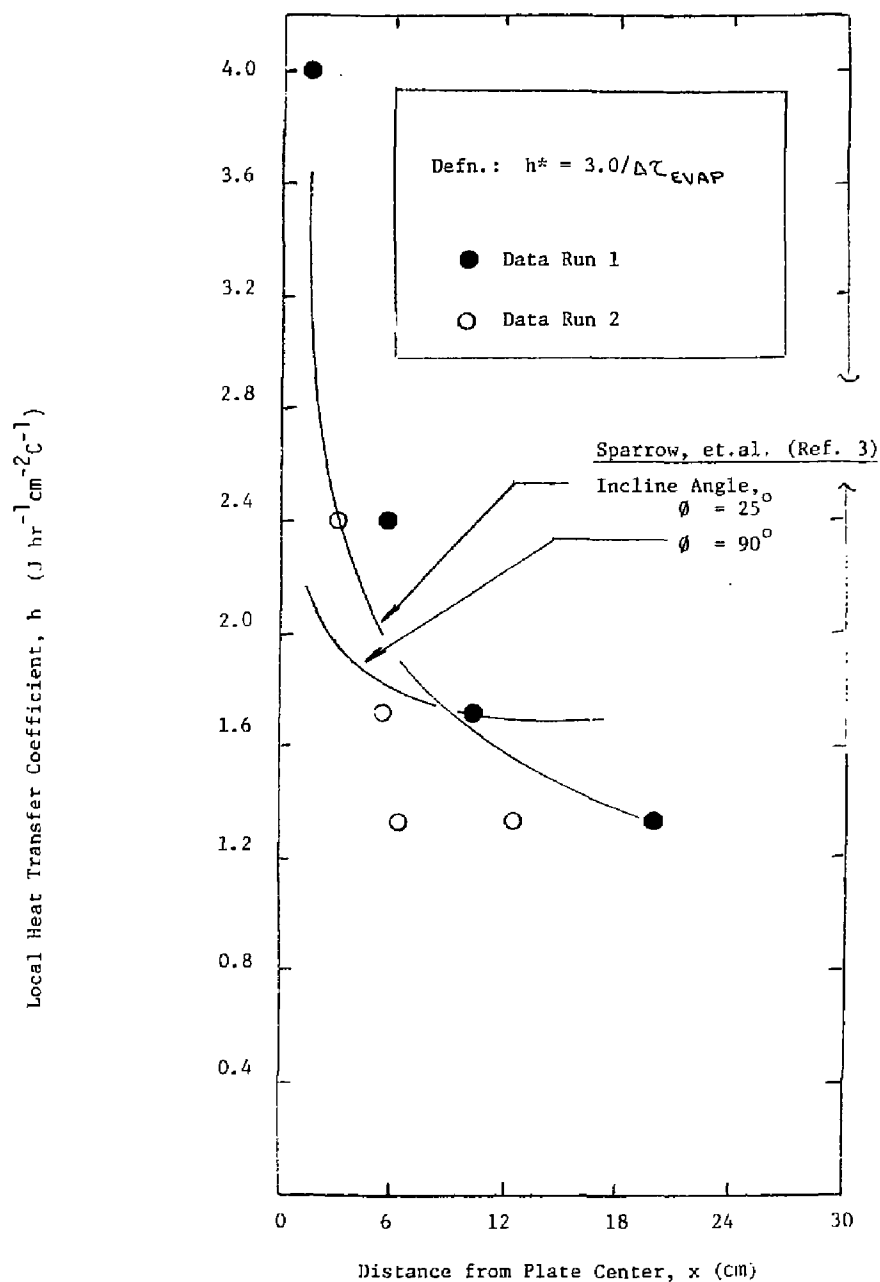
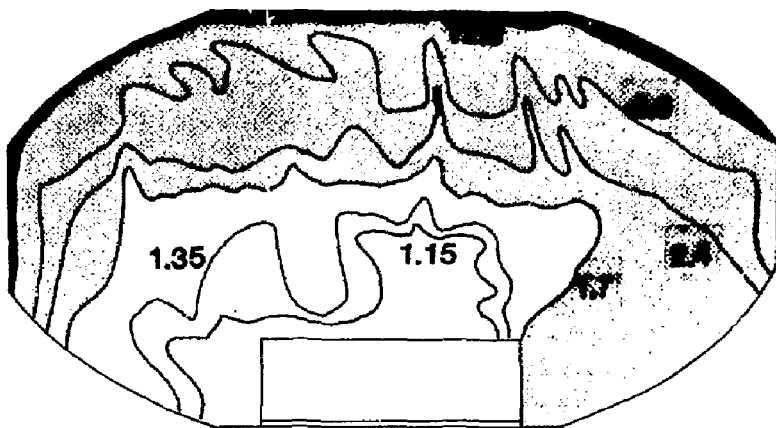


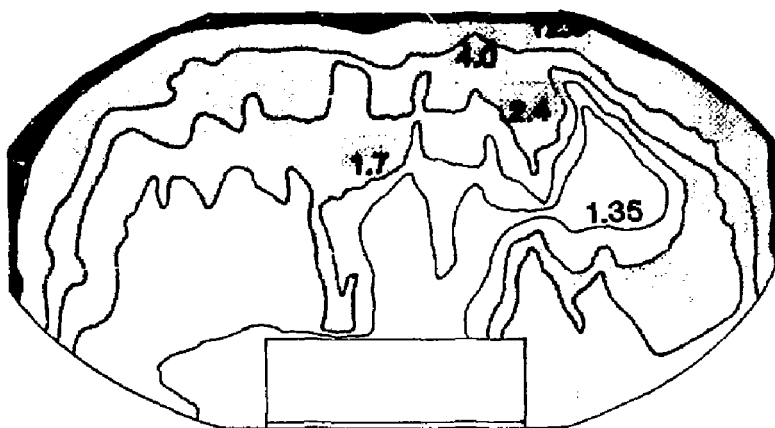
Figure 4.1. Matching of Evaporation Data for Case I with Sparrow Correlation for Flat Plate.

4.4.4.3 Evaporation Measurements

The "China Clay" evaporation data are repeatable as demonstrated by the two deduced variations of convective heat transfer coefficient on the lead disk shown in Figure 4.2. The evaporation data were obtained separately for the baseline flow conditions. The main sources of error in these results are the irregularity of the evaporation patterns which makes it hard to separate evaporated and unevaporated regions and the errors associated with interpreting video tape data. However, the experimenters believe the data are reliable for purposes of developing intrastage hardware.



Run 1



Run 2

Figure 4.2. Comparison of h^* Distribution on Lead Surface of First Disk for Separate Test Runs at the Baseline Flow Condition.

5.0 EXPERIMENTAL RESULTS

Experimental data were taken and reduced as described in Section 4.0. On the basis of the reduced data, experimental results are discussed for each series of tests.

5.1 LAMP CAVITY TESTS

5.1.1 Streakline Data

A number of photographs of bubble streaks in the lamp cavity model were taken. Of these, fifteen were of good quality and could be used for data reduction. As described in Section 4.4.1, a tracing was made of the streaks on a single composite drawing. The following observations were made from the individual photographs, presented in Appendix A, and the composite drawing, presented as Figure 5.1.

1. The streaklines incline slightly upwards toward the exhaust side of the lamp cavity, suggesting the bubbles are not neutral buoyant.
2. The number density of streaklines is uniform over most of the lamp cavity length.
3. The streaks are equally likely to occur in tube interstices and on the tubes.
4. Streakline dashes are longer in tube interstices than over tubes, suggesting acceleration of the flow in between the tubes and the simulated blast shield.

Based on these observations, it is concluded:

1. The straightness of the streaklines implies parallel flow exists in the lamp cavity with the current design of inlet and outlet plenums.

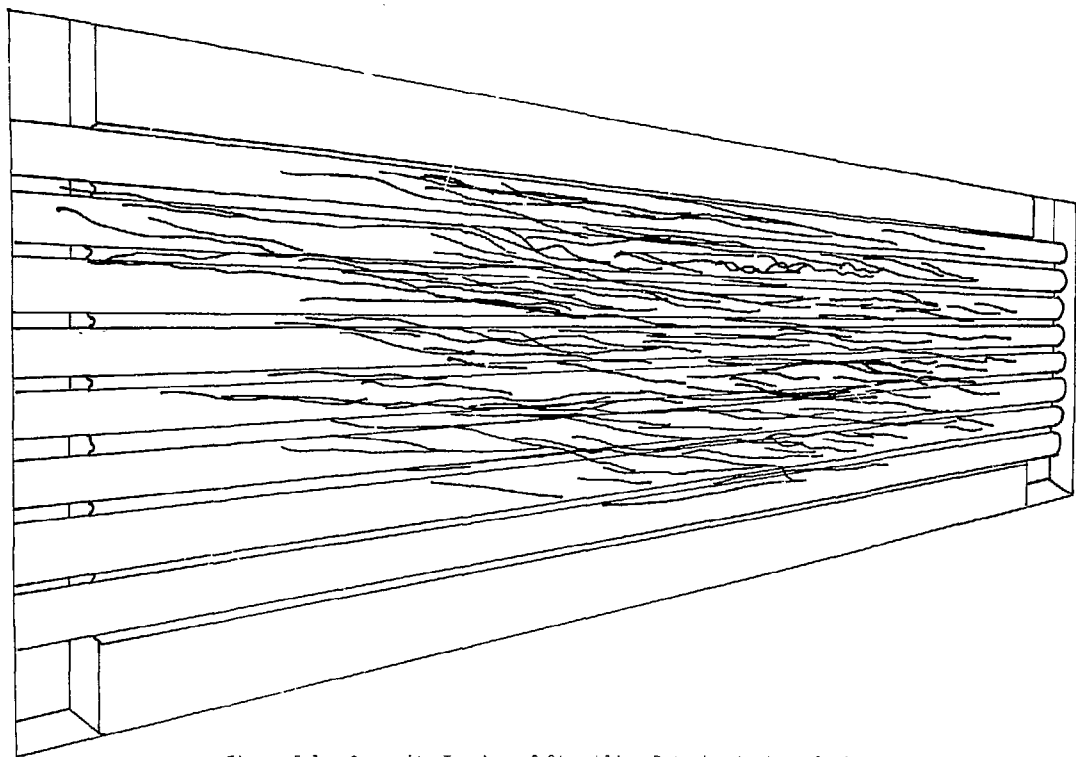


Figure 5.1. Composite Tracing of Streakline Data in the Lamp Cavity
(Flow is Right to Left).

2. The slight upward inclination of the streaklines is most probably caused by bubble buoyancy.
3. Velocity measurements can be easily interrupted and used to establish the degree of flow uniformity in the cavity.

5.1.2 Velocity Measurements

Velocity measurements were made across the lamp cavity at three axial locations: near the inlet, at midlength and near the exhaust. Data at three measurement depths were obtained and are presented in Figure 5.2. The following observations can be made.

1. The maximum point-to-point velocity variations at each depth are:
 - Inlet axial position: 70%
 - Midlength axial position: 10%
 - Exhaust axial position: 30%
2. Maximum velocity variation with depth is about 30%.
3. At the upstream axial position, there is near stagnant flow at the center lamp position.

The trend of the velocity data corroborates the results of the flow visualization experiments.

Based on these observations, it is concluded:

1. With the exception of the most upstream location, there are no regions of flow stagnation in the lamp cavity and the plenum designs are acceptable.
2. The flow through the lamp cavity is essentially parallel.

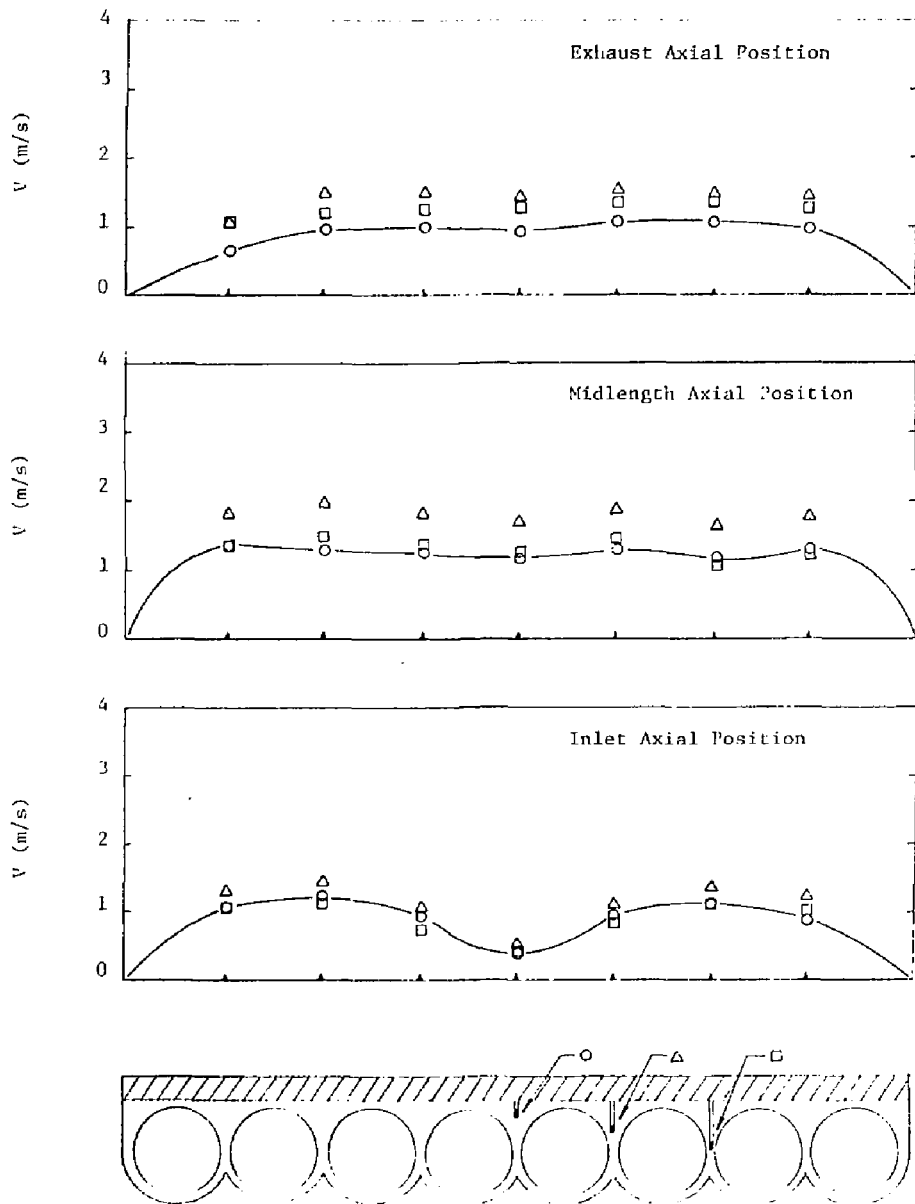


Figure 5.2. Measured Gas Velocities in Simulated 20.8-cm Nova Amplifier Lamp Cavity.

3. The small velocity variation with depth that exists between the tubes implies there is no stagnant region near the tubes or reflector and convective cooling of the lamp cavity is near optimum.

5.2 DISK CAVITY TESTS

5.2.1 Streakline Data

Figure 5.3 is representative of the photograph taken at the first upstream disk for the baseline flow condition. These photographs are poor in quality and difficult to interpret. However, streaklines observed on both sides of the upstream disk vary irregularly and do suggest that the flow is very low in velocity and highly disordered. Because of the poor quality of these data, the influence of inlet plenum designs must be evaluated solely on the basis of measured evaporation rates.

5.2.2 Evaporation Data on Laser Disk Surfaces

Three candidate intrastage hardware configurations were evaluated in these tests. The corresponding test cases are:

- Case I: Baseline configuration where the inner liner, shown in Figure 3.7, is removed and the vaned air channel is circumvented.
- Case II: Configuration where channel vanes are aligned with the disk cavity axis simulating an unswirled flow condition.
- Case III: Configuration where channel vanes are turned 45° to the disk cavity axis, simulating a fully-swirled flow condition.

Evaporation rates were measured on the first upstream disk in all cases for comparative purposes. Evaporation rates were also measured on

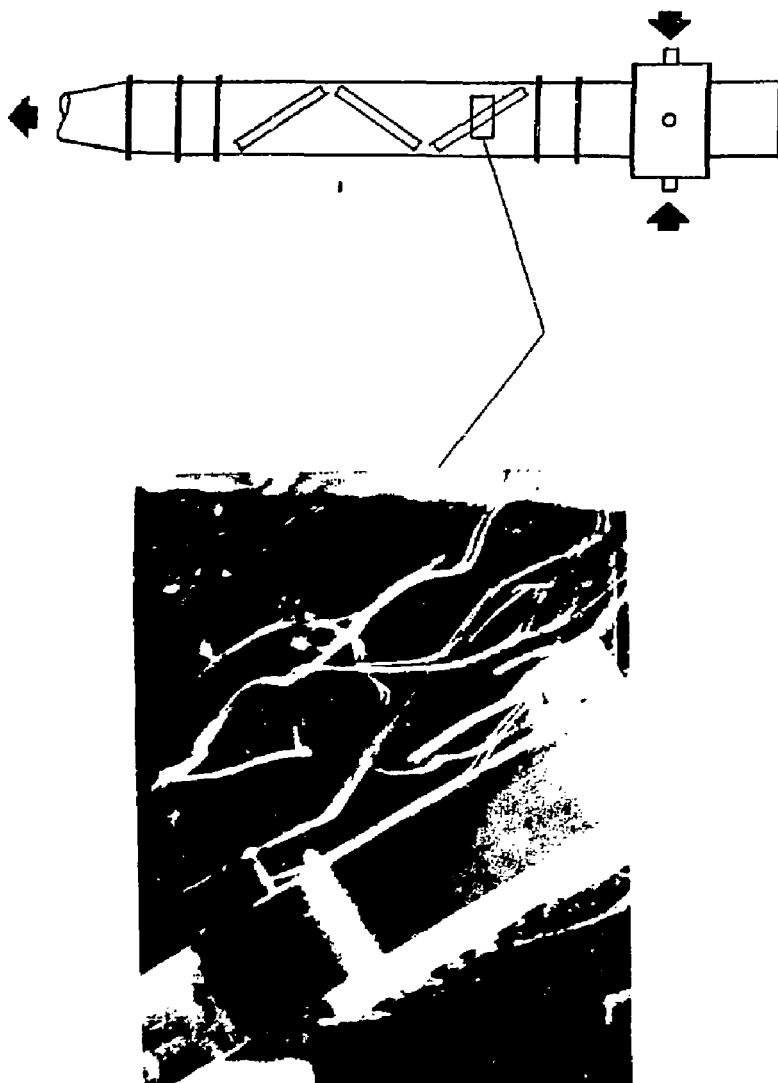


Figure 5.3. Representative Streakline Data (Run 3) Obtained at First Disk for Baseline Flow Condition.

surfaces of the other two disks in Case I, after this intrastage hardware configuration was judged best of the three configurations considered. All data are reported in Appendix B.

5.2.2.1 Comparison of First Disk Measurements

Figure 5.4[†] through 5.6 present contours of the convective heat transfer coefficient h^* on the first disk for Cases I, II, and III, respectively. The following observations can be made.:

1. Comparison of Cases I and II suggest use of a vaned flow channel can achieve a more uniform distribution of convective heat transfer on the lead disk surface but at the expense of a reduced heat transfer rate.
2. Comparison of Cases I and III suggest swirling the flow by means of turning the flow channel vanes can be used to enhance the heat transfer rate but the distribution is similar to that achieved with the simple hardware in Case I.
3. In all cases, the convective heat transfer coefficients are lowest near the disk mounting location where flow around the disk edge is blocked.

Based on these observations, it was concluded that the simple hardware configuration of Case I should be adopted for the Nova box amplifier. Of particular importance, is the cost savings achieved by eliminating the conceived vaned flow channel that does not significantly improve the flow condition according to the present test.

[†]Labels of contours on the downstream surfaces are left upside down to facilitate cut out of the plots and construction of 3-dimensional laser disks to be placed in a 3-dimensional representation of the disk cavity.

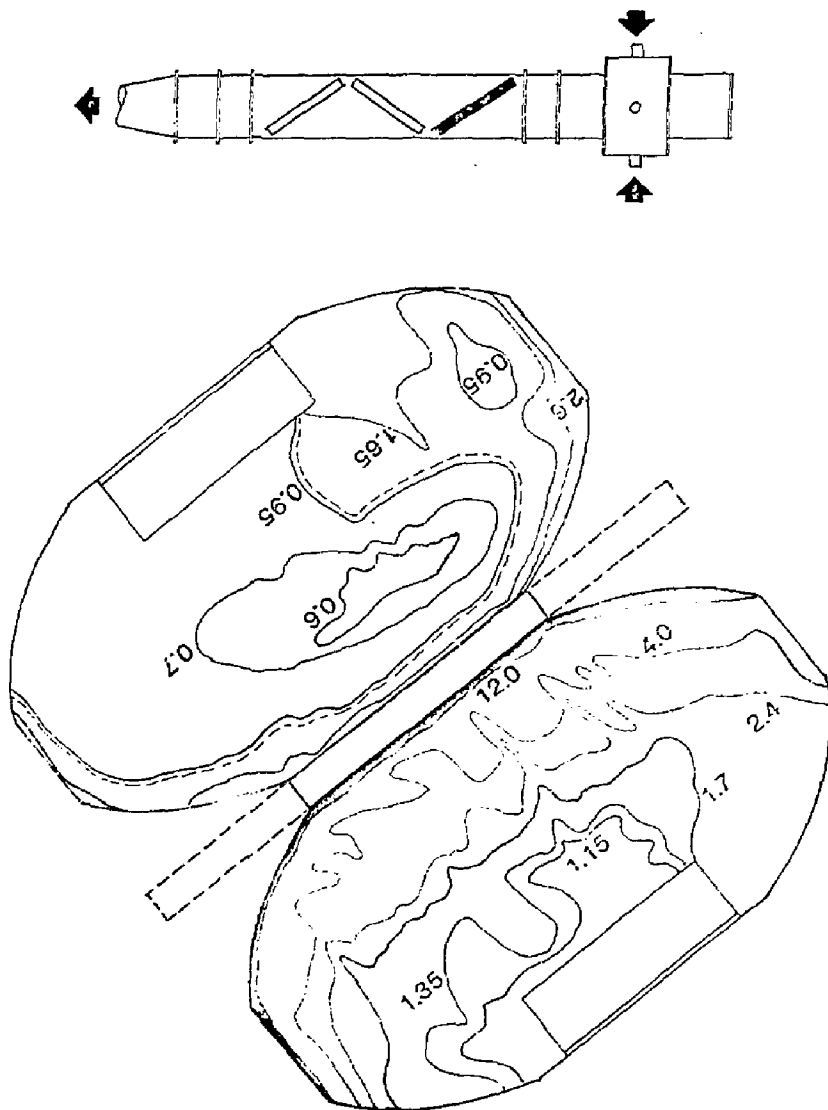


Figure 5.4. Case I - No Inner Liner: Distribution of h^* on Surfaces of First Laser Disk (Run 1).

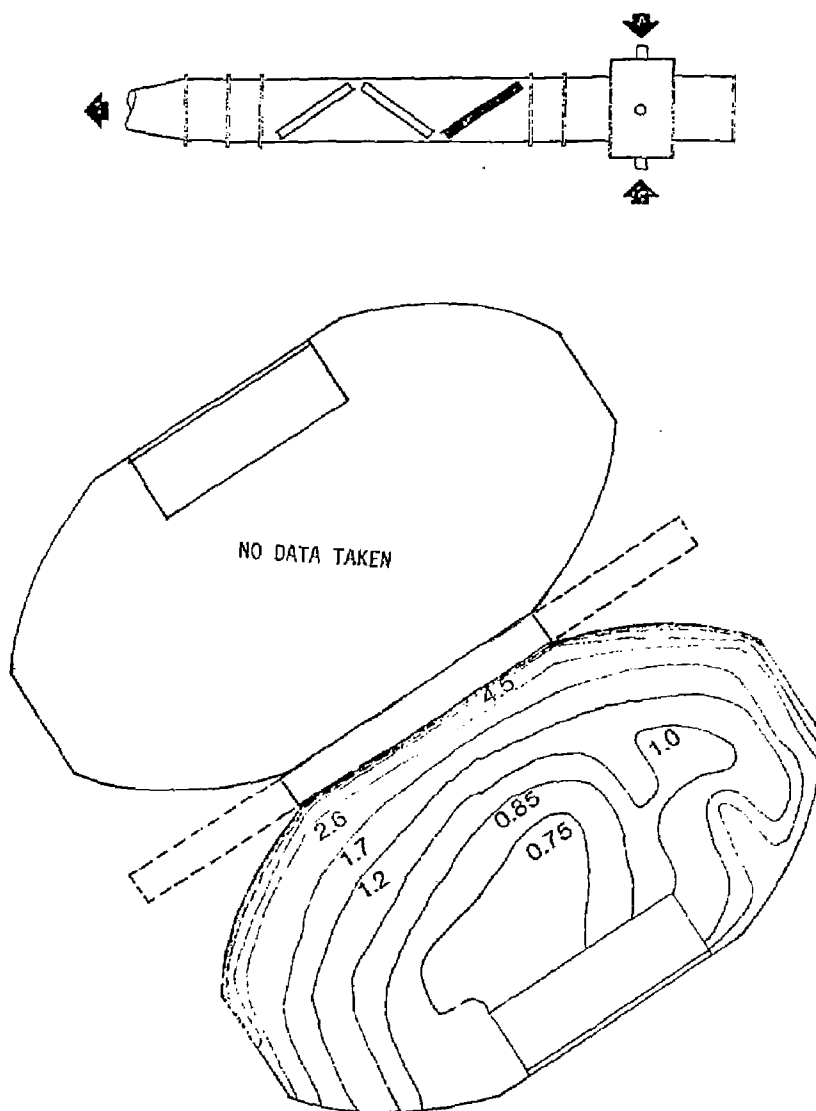


Figure 5.5. Case II - Plenum with Vanes at 0° : Distribution of h^* on Surfaces of First Laser Disk.

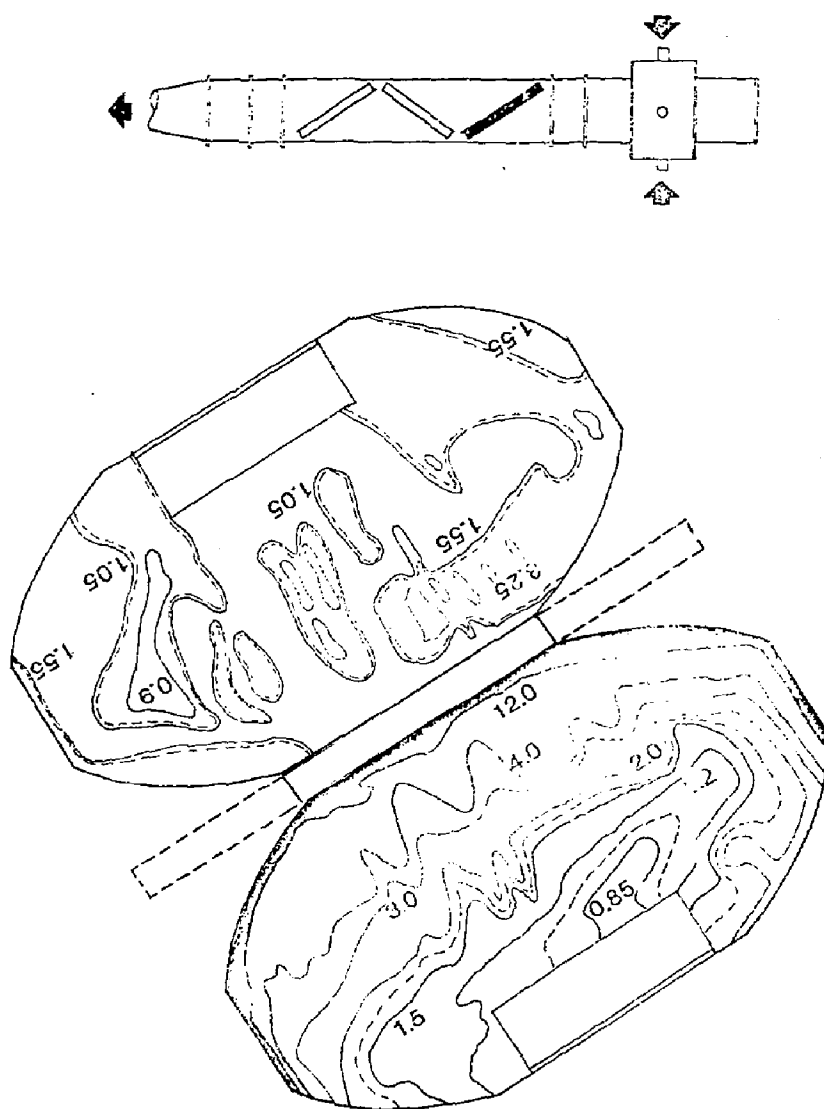


Figure 5.6. Case III - Plenum with Vanes at 45° : Distribution of h^* on Surfaces of First Laser Disk.

5.2.2.2 Measurements on All Disks Surfaces for Case I

Figures 5.7 and 5.8 present contour of h^* on the second and third disks for Case I, respectively. Comparison of these results with those obtained on the first disk, presented in Figure 5.4, suggests:

1. The distribution of convective heat transfer coefficient is highly nonuniform on all disk surfaces.
2. Overall convective cooling is comparable for each disk surface even though the local rates of cooling are different.

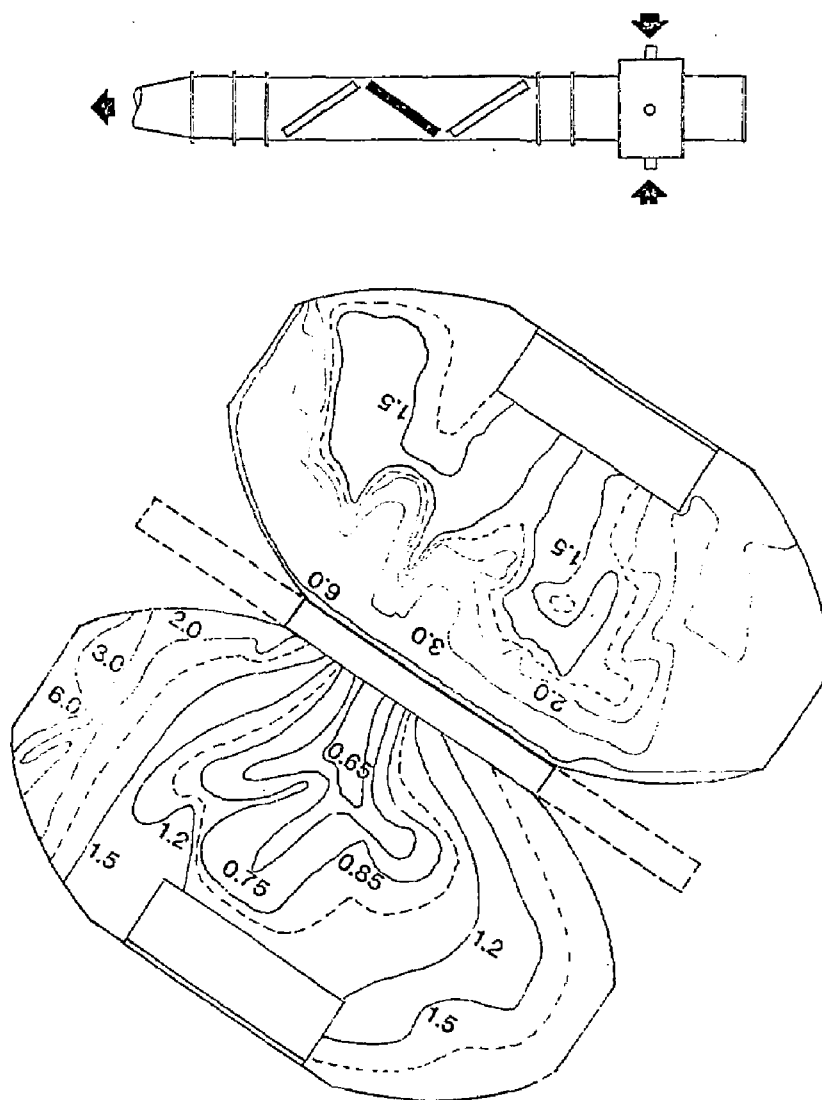


Figure 5.7. Case I - No Inner Liner: Distribution of h^* on Surfaces of Second Laser Disk.

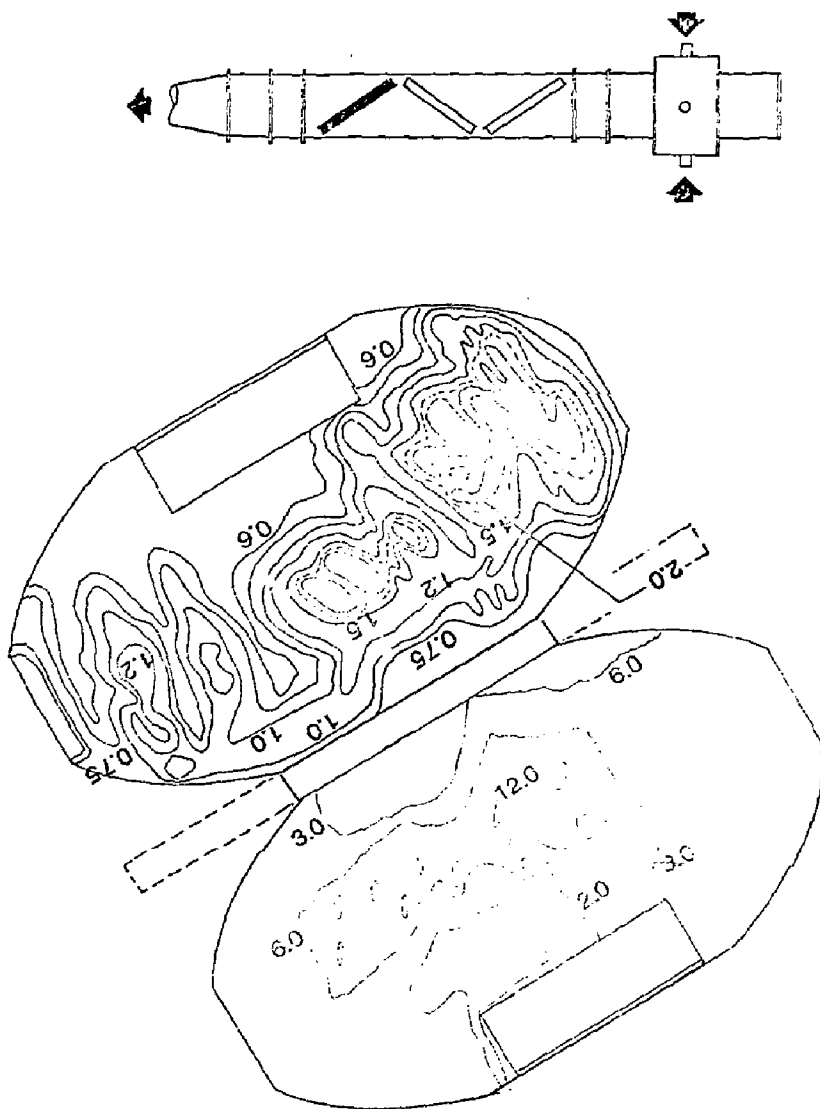


Figure 5.8. Case I - No Inner Liner: Distribution of h^* on Surfaces of Third Laser Disk.

REFERENCES

1. H. L. Julien, "Conduction, Convection, and Radiant Energy Exchange during Convective Cooling of Glass Laser Disks", LLNL Memorandum Nova 80-808, October 1980.
2. E. L. Molishever, "Convective Cooling of Nova Box Amplifiers", LLNL Memorandum Nova 81-440, August 1981.
3. E. M. Sparrow, J. W. Ramsey and E. A. Mass, "Effect of Finite Width on Heat Transfer and Fluid Flow about an Inclined Rectangular Plate", ASME Journal of Heat Transfer, May 1979.

APPENDIX A RECORDED STREAKLINE DATA

Fifteen photographs (Figures A.1 - A.15) of recorded streakline data in the lamp cavity model are shown here. They were all taken at a design flowrate equal to 6 cfm. The composite drawing, presented as Figure 5.1, was constructed by superimposing in one tracing the steaklines from these fifteen photographs.

Six photographs (Figures A.16 - A.21) of recorded streakline data in the disk cavity model are also shown. These data were taken at a design flowrate equal to 18 cfm.

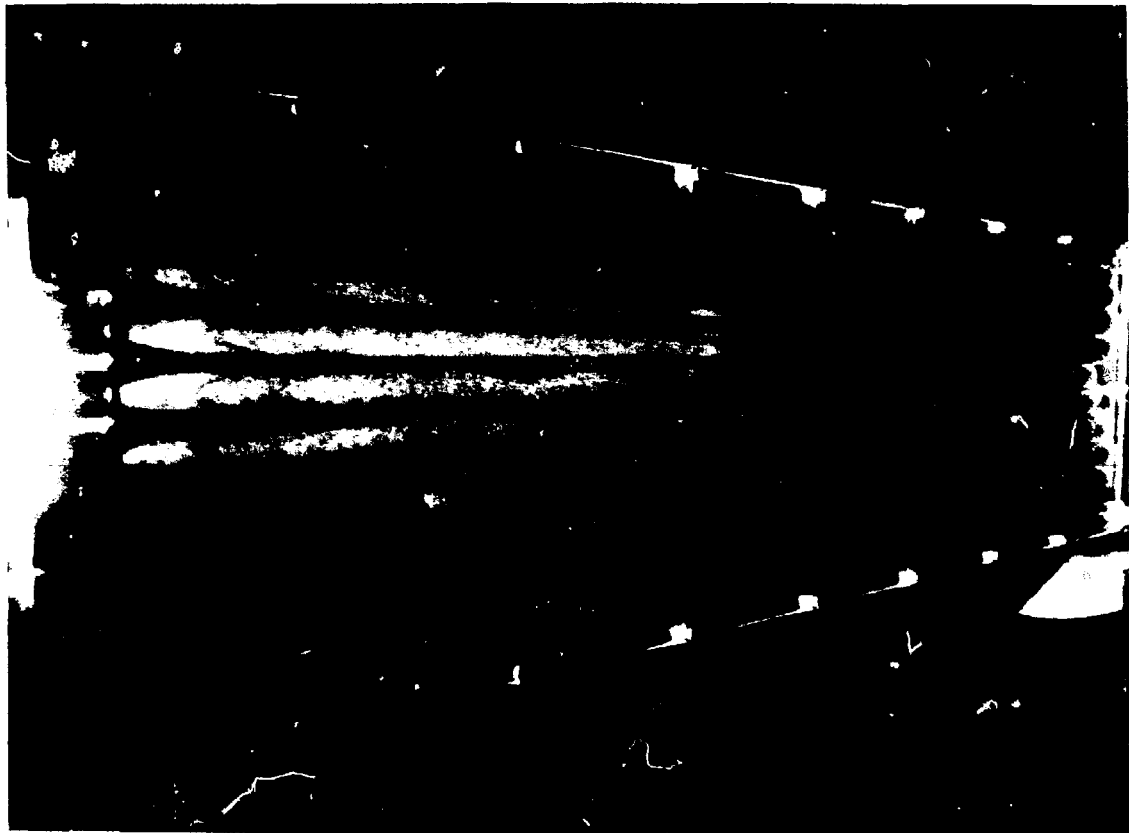


Figure A.1. Observed Streaklines in Lamp Cavity Model: Run 1 (Flow Right to Left).

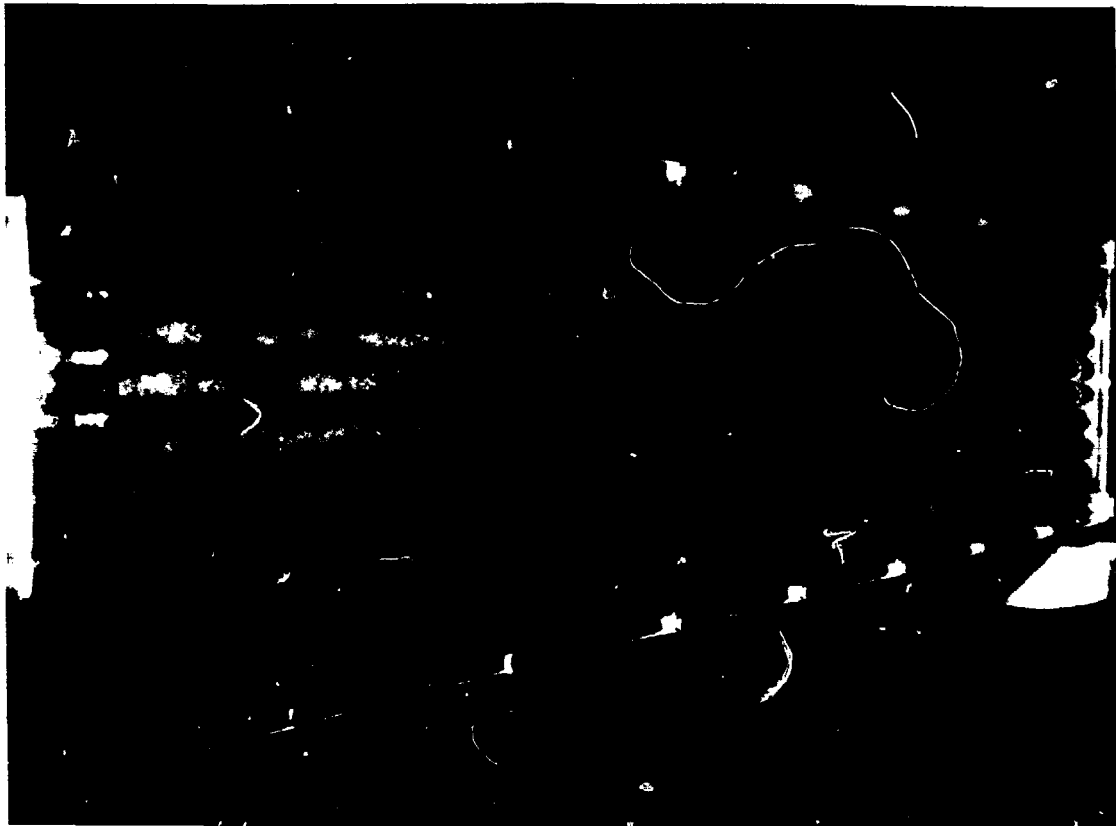


Figure A.2. Observed Streaklines in Lamp Cavity Model: Run 2 (Flow Right to Left).

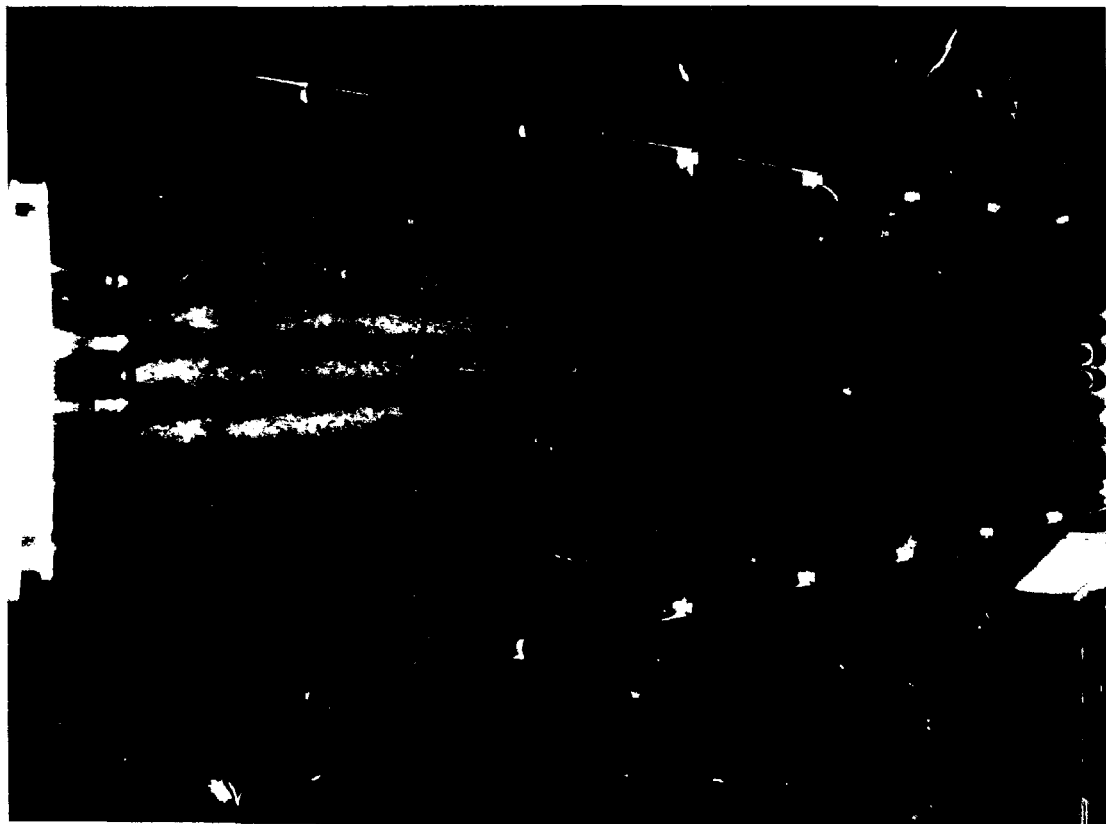


Figure A.3. Observed Streaklines in Lamp Cavity Model: Run 3 (Flow Right to Left).

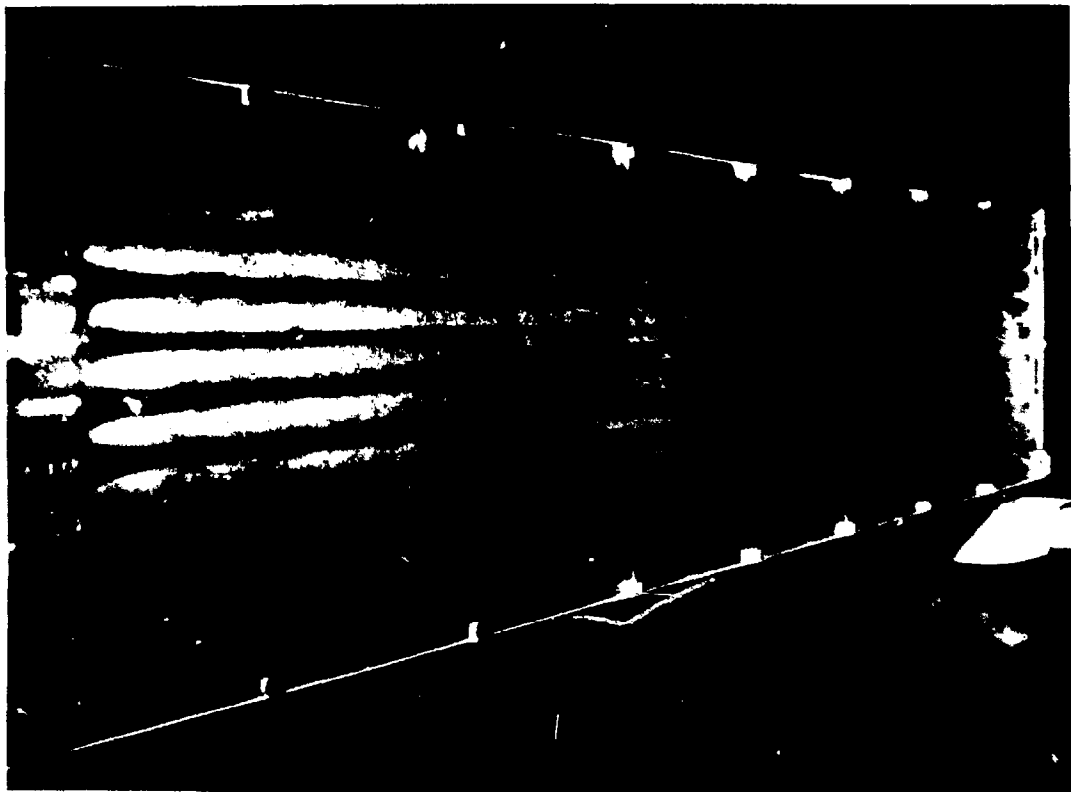


Figure A.4. Observed Streaklines in Lamp Cavity Model: Run 4 (Flow Right to Left).

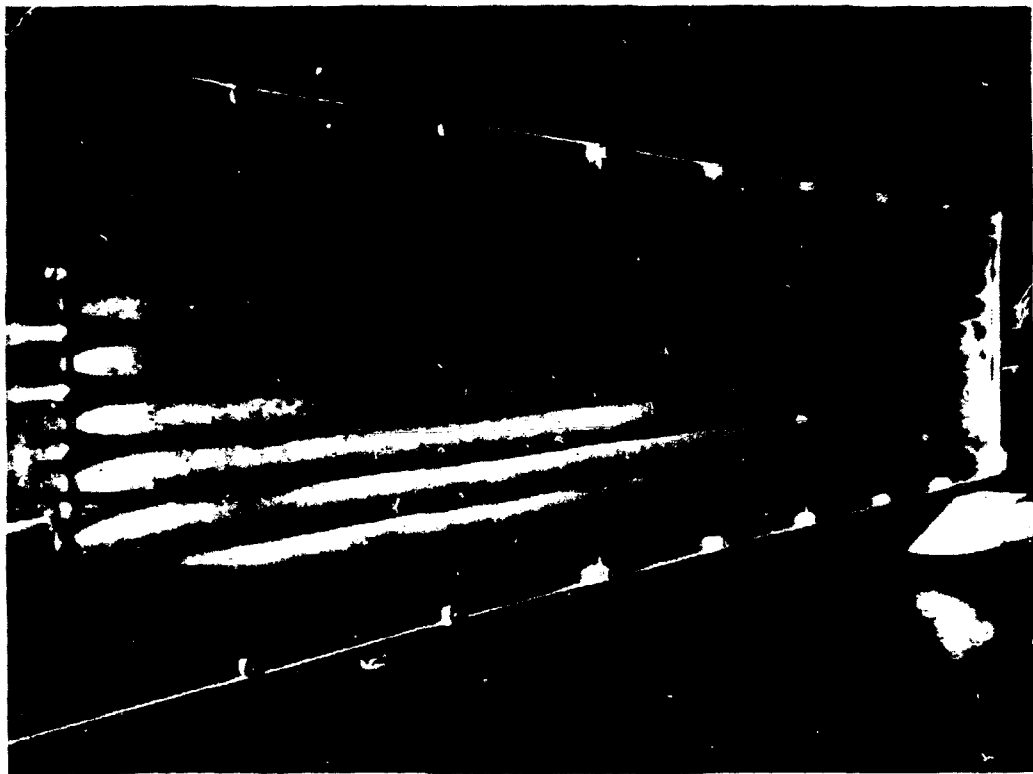


Figure A.5. Observed Streaklines in Lamp Cavity Model: Run 5 (Flow Right to Left).

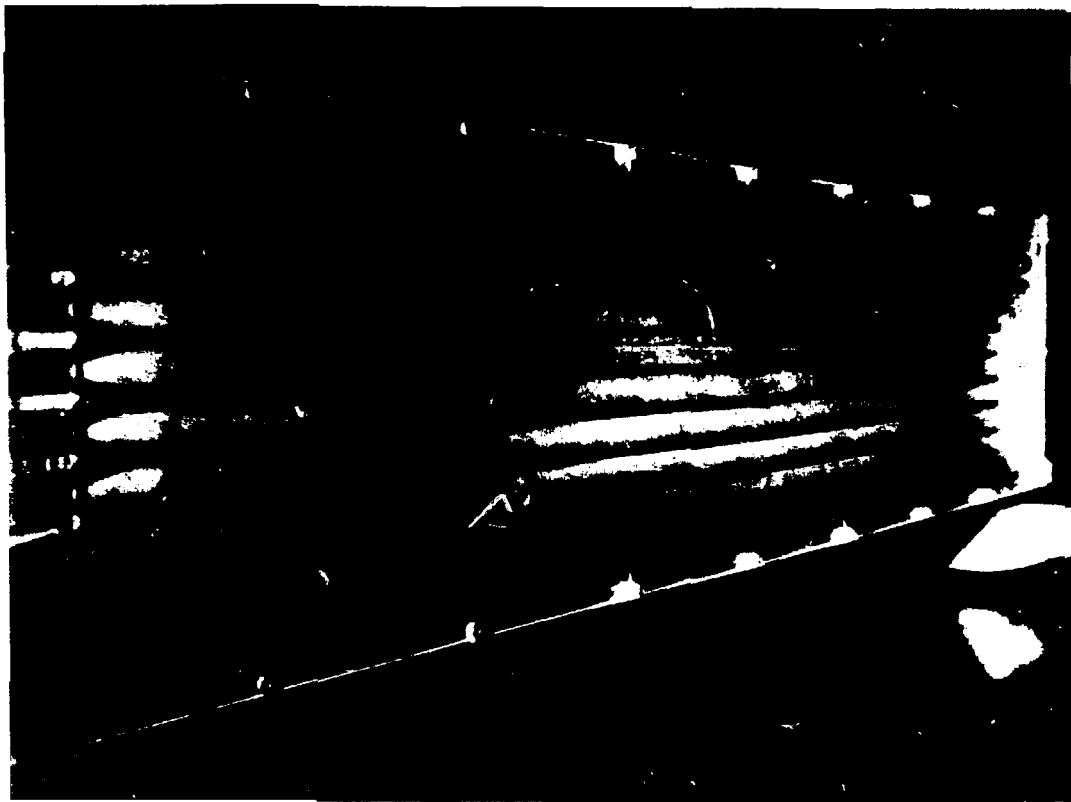


Figure A.6. Observed Streaklines in Lamp Cavity Model: Run 6 (Flow Right to Left).



Figure A.7. Observed Streaklines in Lamp Cavity Model: Run 7 (Flow Right to Left).

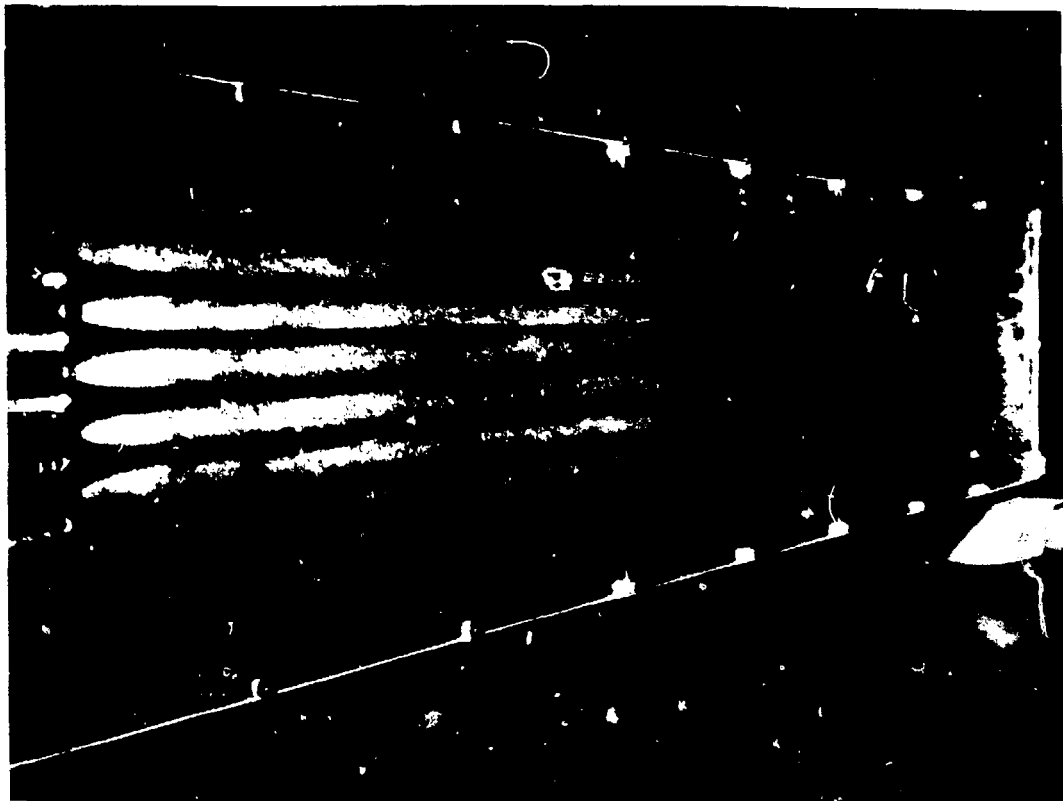


Figure A.8. Observed Streaklines in Lamp Cavity Model: Run 8 (Flow Right to Left).

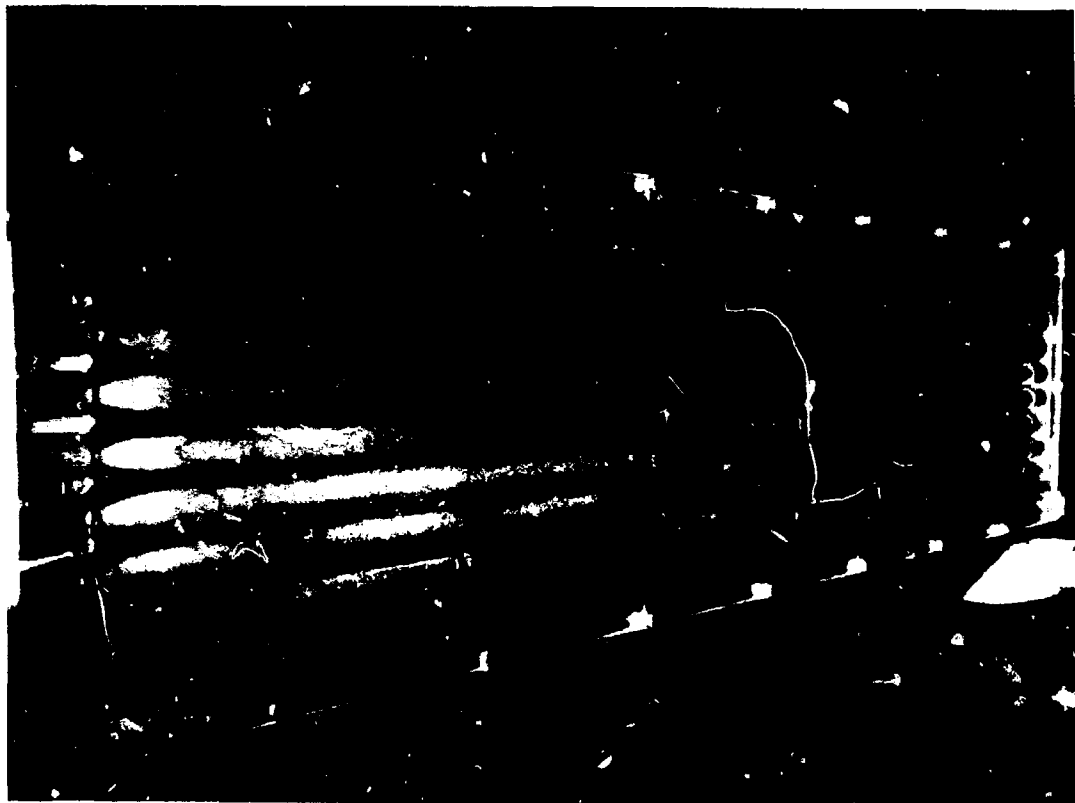


Figure A.9. Observed Streaklines in Lamp Cavity Model: Run 9 (Flow Right to Left).

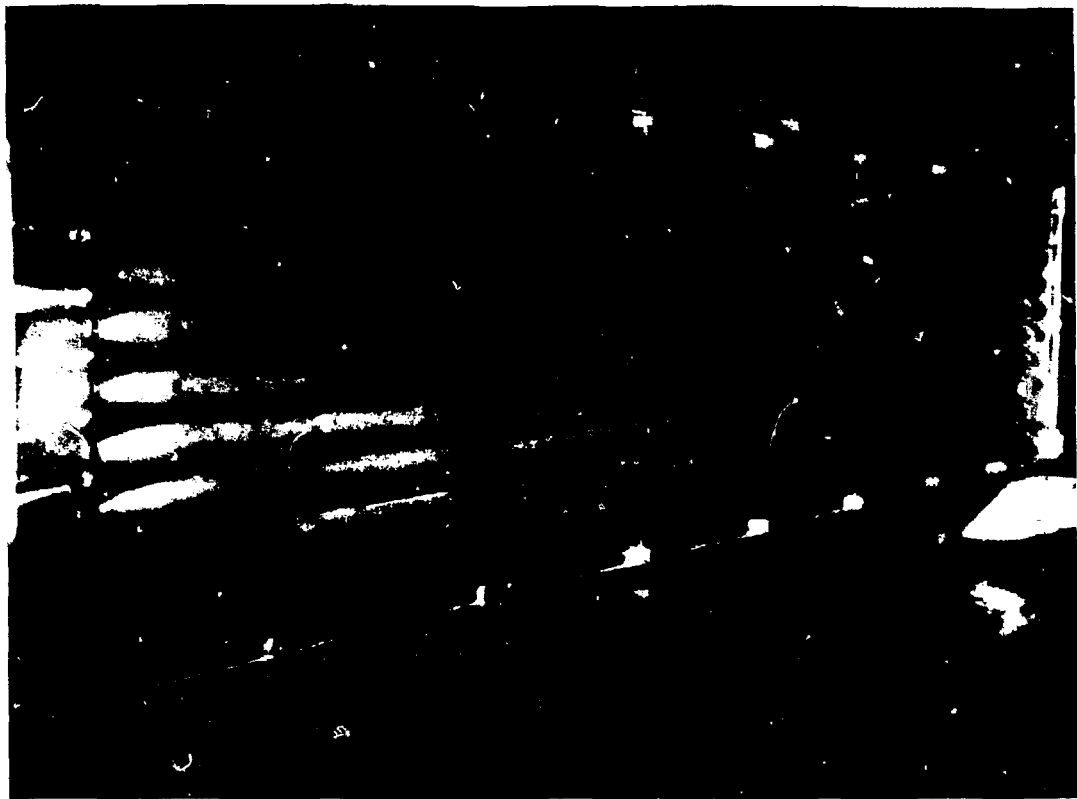


Figure A.10. Observed Streaklines in Lamp Cavity Model: Run 10 (Flow Right to Left).

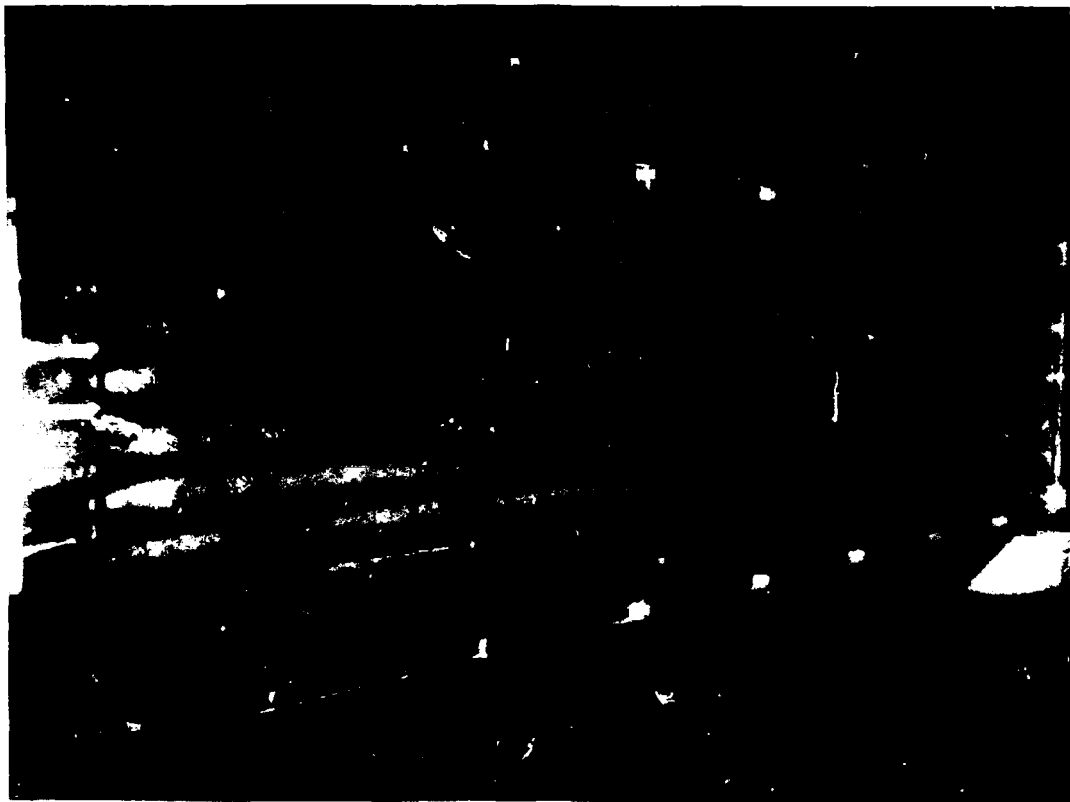


Figure A.11. Observed Streaklines in Lamp Cavity Model: Run 11 (Flow Right to Left).

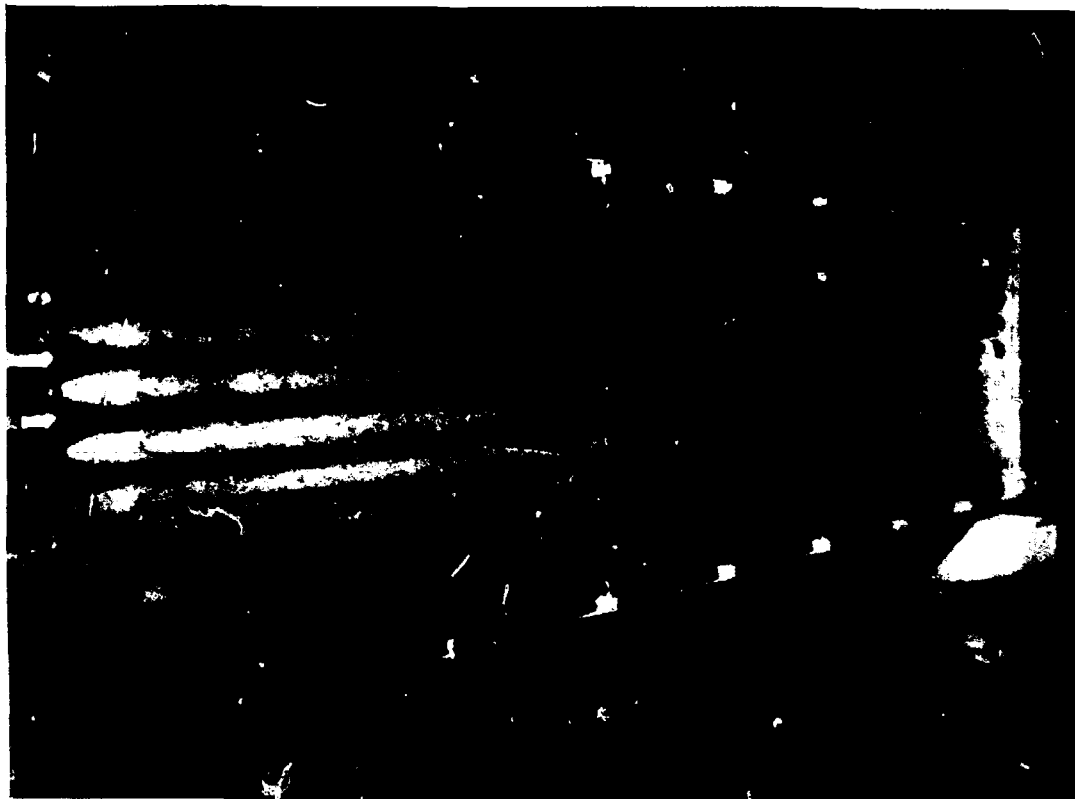


Figure A.12. Observed Streaklines in Lamp Cavity Model: Run 12 (Flow Right to Left).

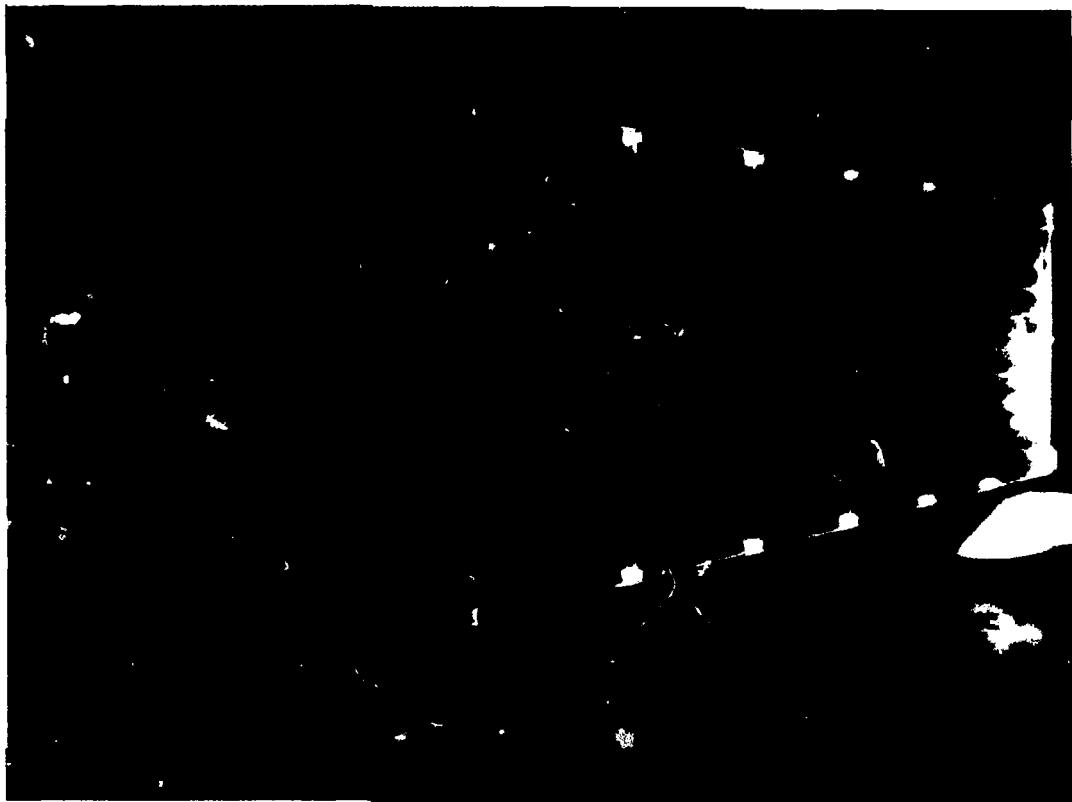


Figure A.13. Observed Streaklines in Lamp Cavity Model: Run 13 (Flow Right to Left).

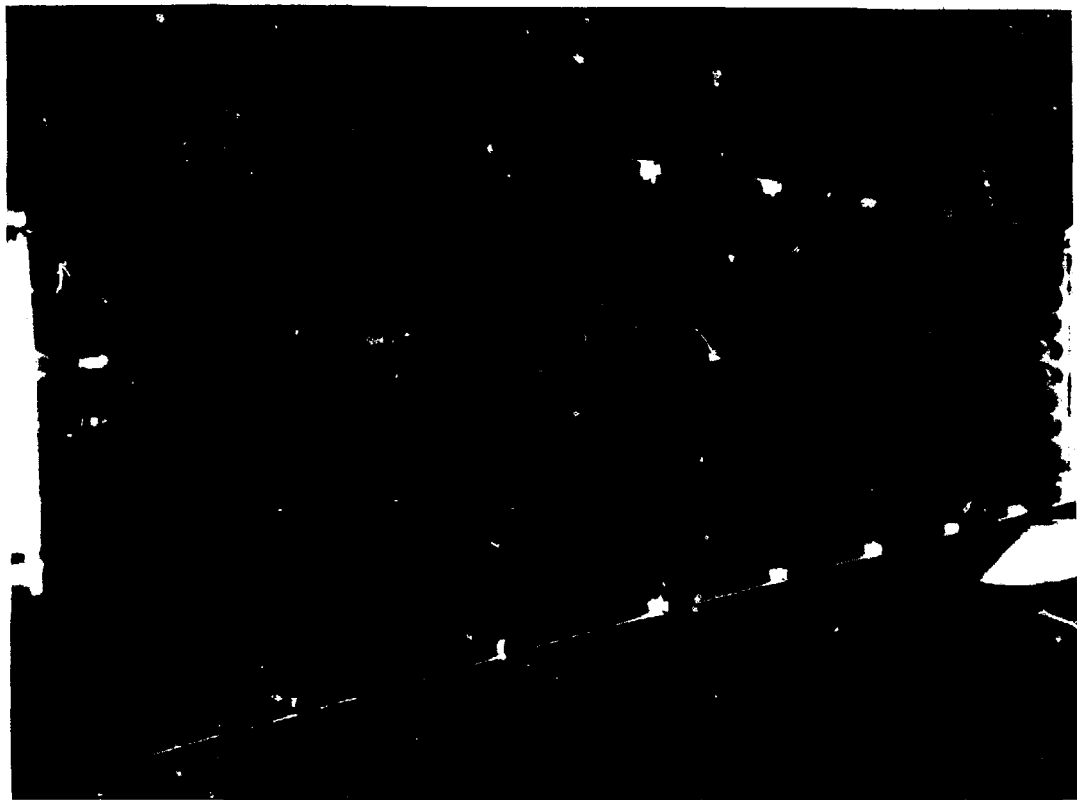


Figure A.14. Observed Streaklines in Lamp Cavity Model: Run 14 (Flow Right to Left).

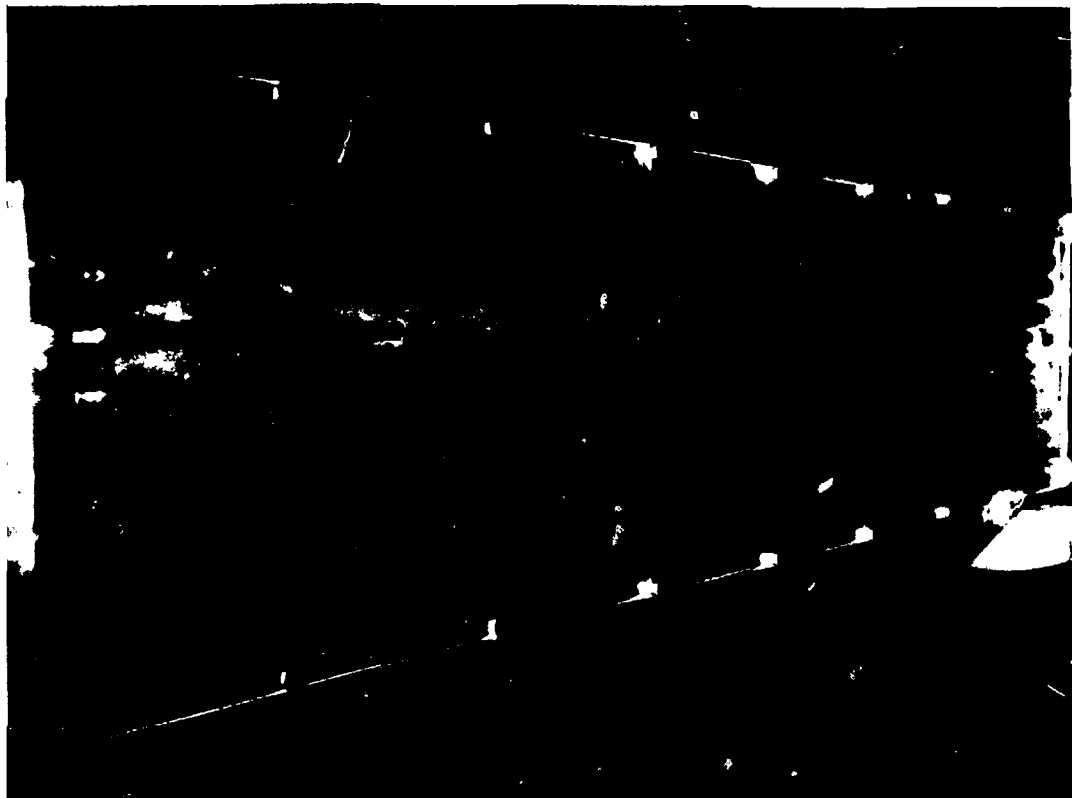


Figure A.15. Observed Streaklines in Lamp Cavity Model: Run 15 (Flow Right to Left).

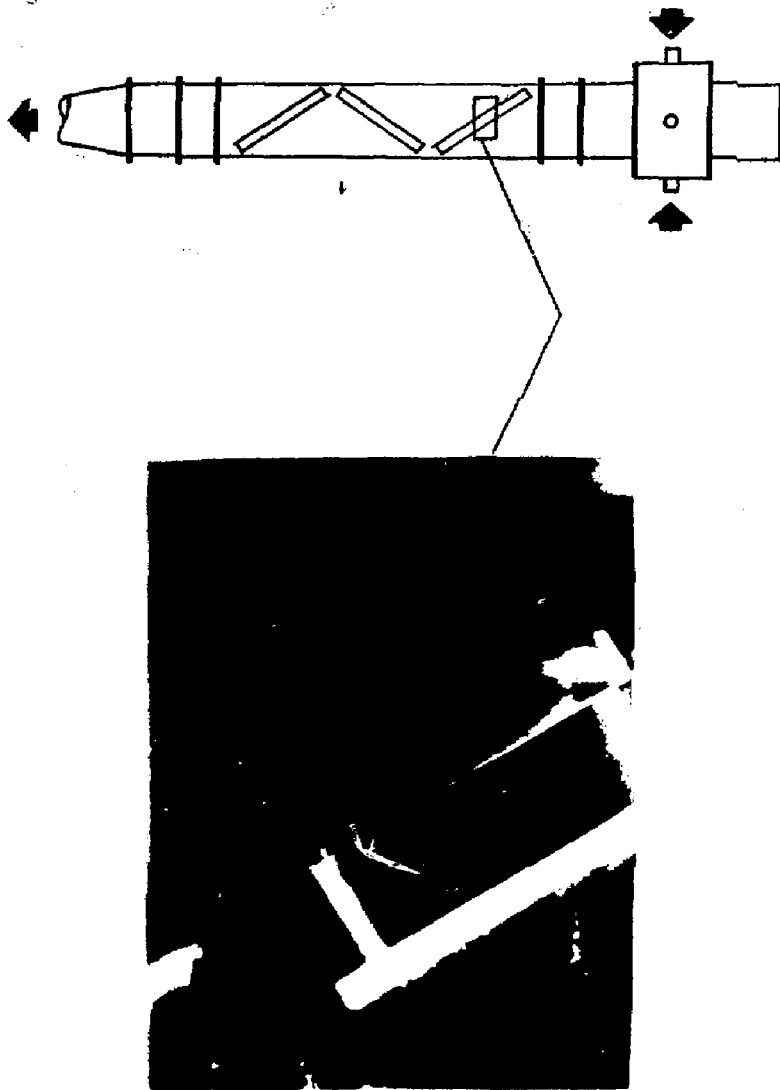


Figure A.16. Case I - No Inner Liner: Observed Streaklines at First Disk in Disk Cavity Model (Run 1).

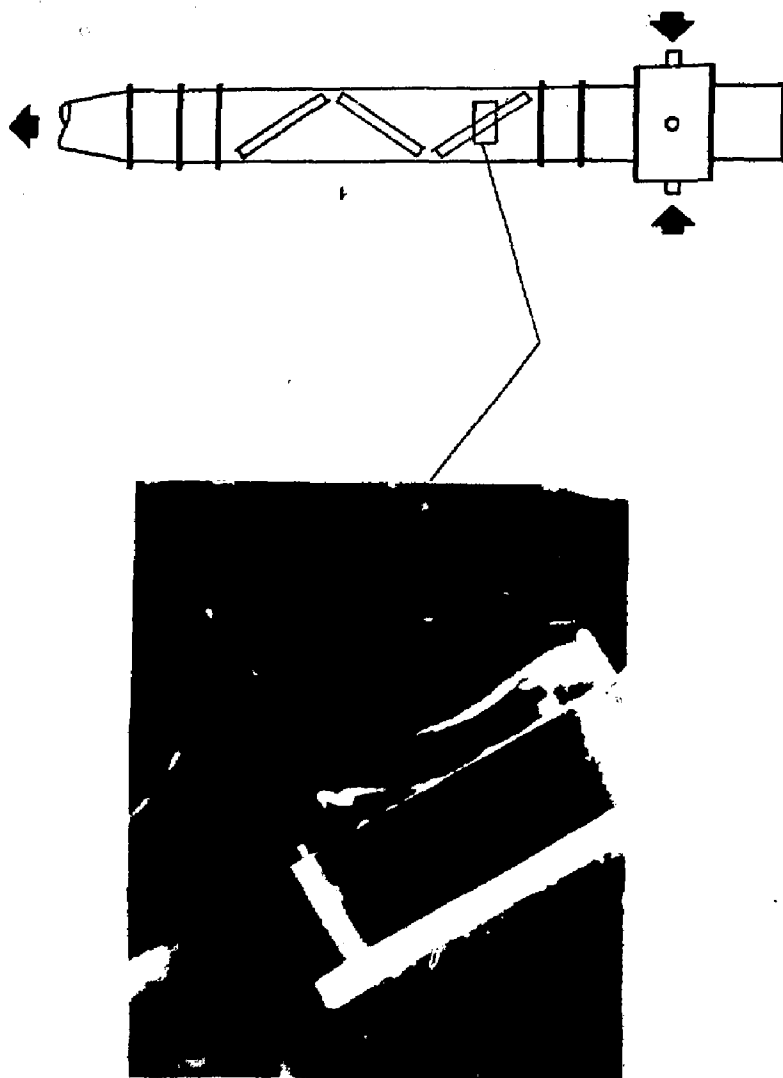


Figure A.17. Case I - No Inner Liner; Observed Streaklines at First Disk in Disk Cavity Model (Run 2).

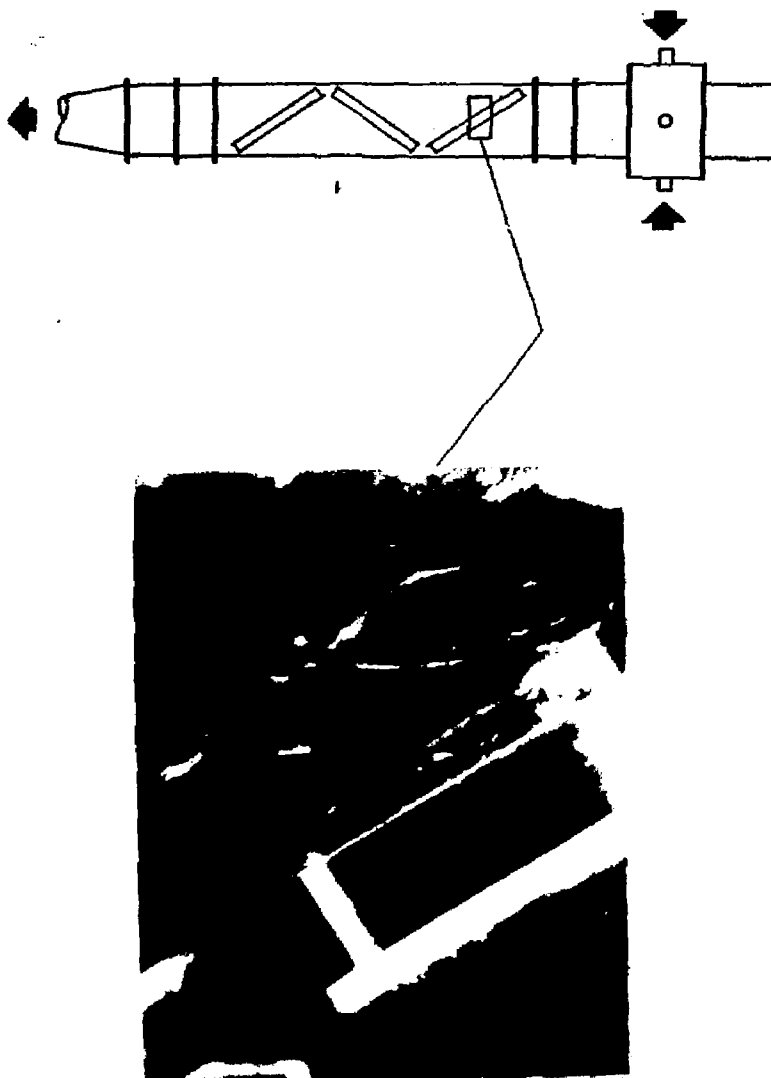


Figure A.18. Case I - No Inner Liner; Observed Streaklines at First Disk in Disk Cavity Model (Run 3).

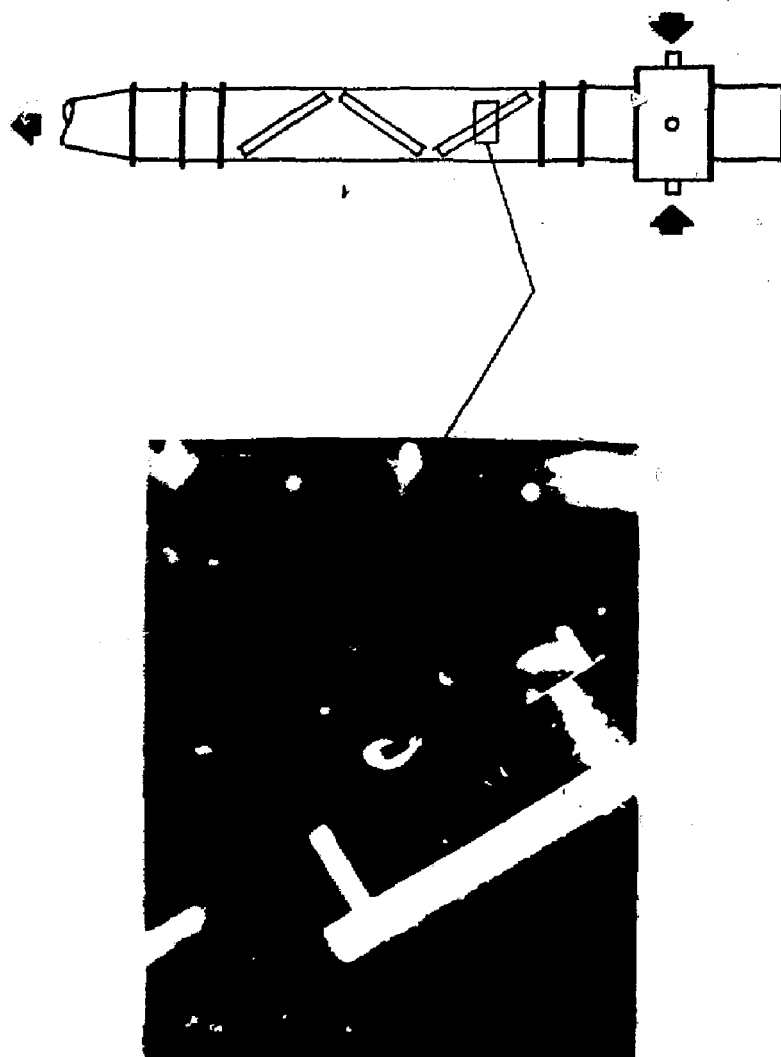


Figure A.19. Case I - No Inner Liner; Observed Streaklines at First Disk in Disk Cavity Model (Run 4).

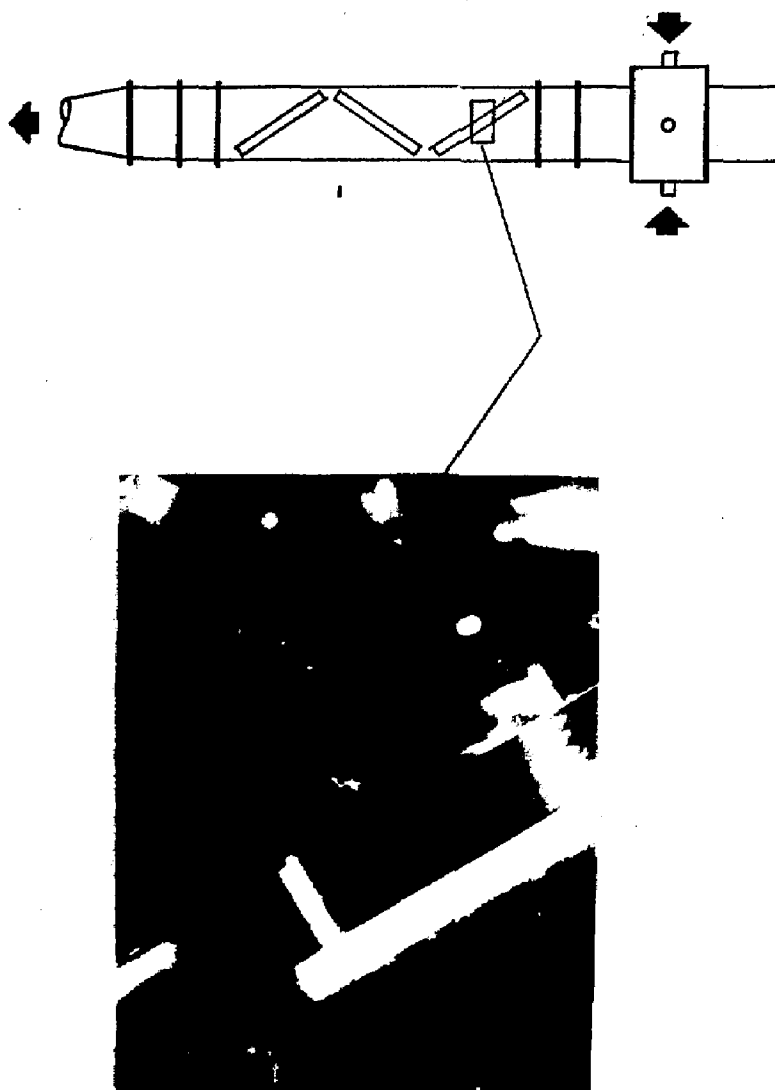


Figure A.20. Case I - No Inner Liner: Observed Steaklines at First Disk in Disk Cavity Model (Run 5).

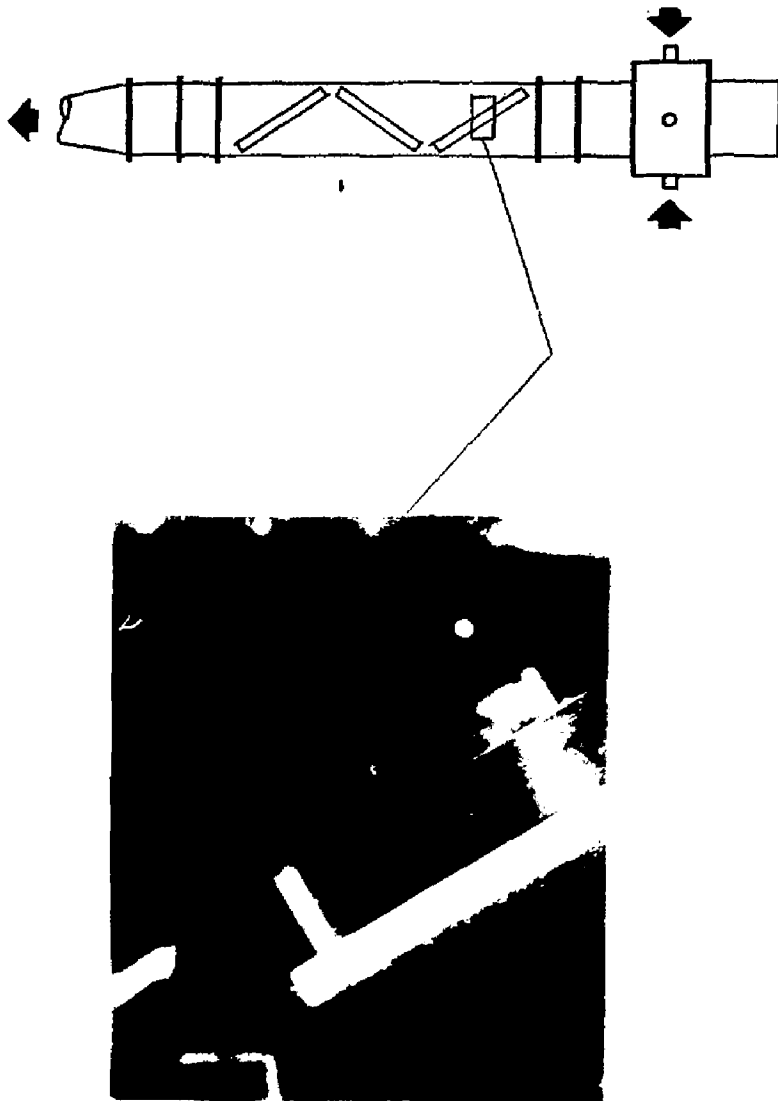


Figure A.21. Case I - No Inner Liner: Observed Streaklines at First Disk in Disk Cavity Model (Run 6).

APPENDIX B MEASURED EVAPORATION RATES AT LASER DISK SURFACES

The spatial variation of convective heat transfer coefficient deduced from evaporation data are shown in Figures B.1 - B.10.

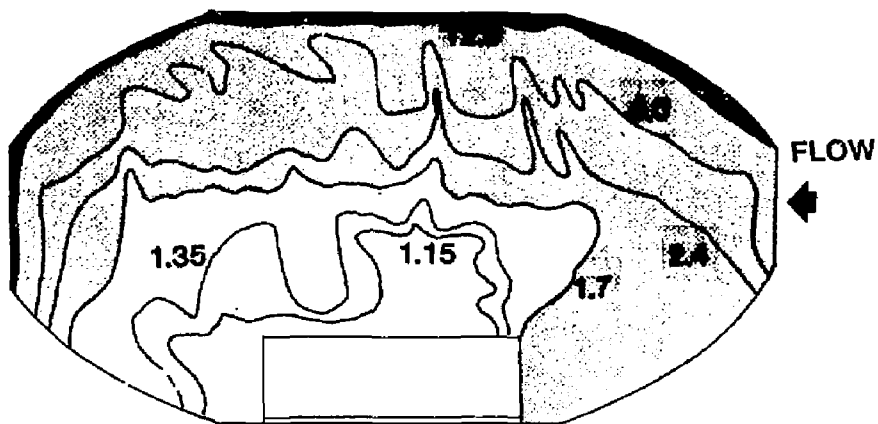
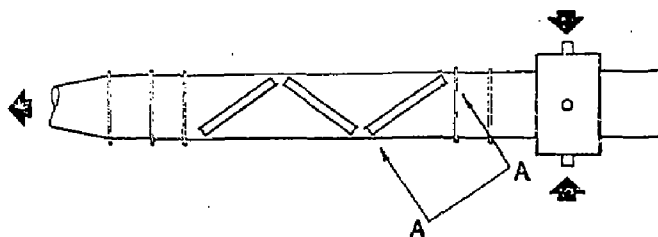
The cases covered are:

Case I: Baseline configuration of inlet intrastage hardware where the inner liner is removed and the vaned air channel is circumvented.

Case II: Configuration where channel vanes are aligned with the disk cavity axis, simulating an unswirled flow condition.

Case III: Configuration where channel vanes are turned 45° to the disk cavity axis, simulating a fully-swirled flow condition.

Results are presented for Case I, followed by results for Cases II and III. In Case I, distributions on the first upstream disk are followed by distributions on the second and third downstream disks. In Cases II and III, distributions are presented for the first upstream disk only.



SECTION A-A

Figure B.1. Case I - No Inner Liner: Distribution of h^* on Front Surface of First Laser Disk (Run 1).

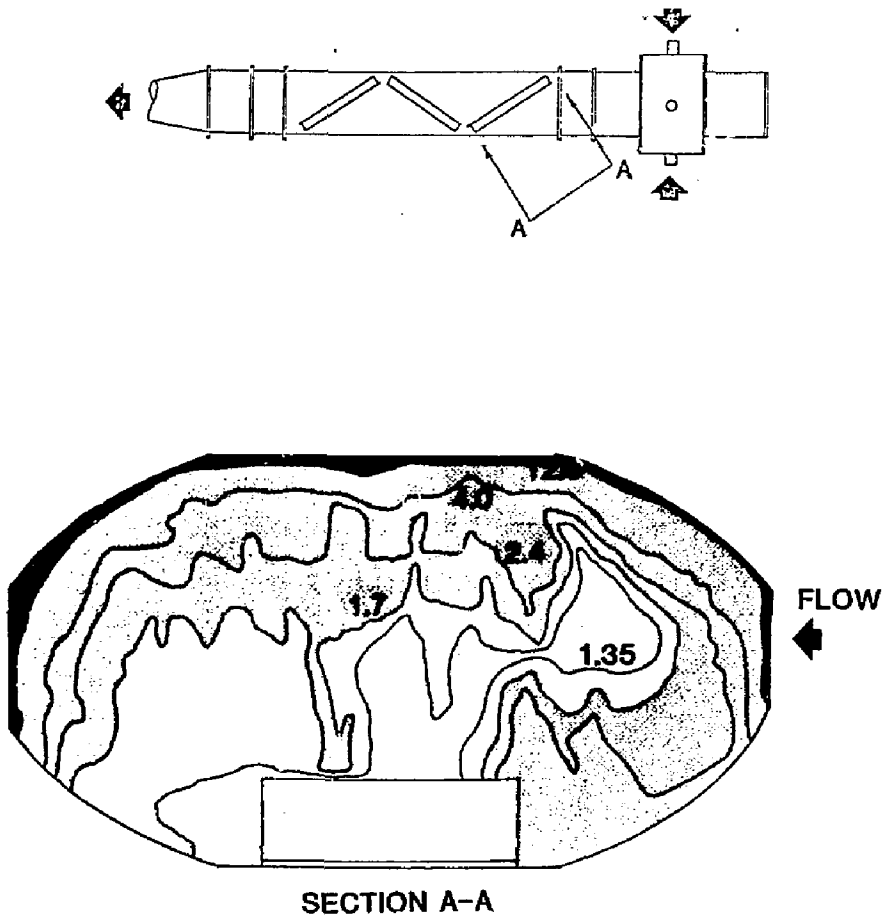


Figure B.2. Case I - No Inner Liner: Distribution of h^* on Front Surface of First Laser Disk (Run 2).

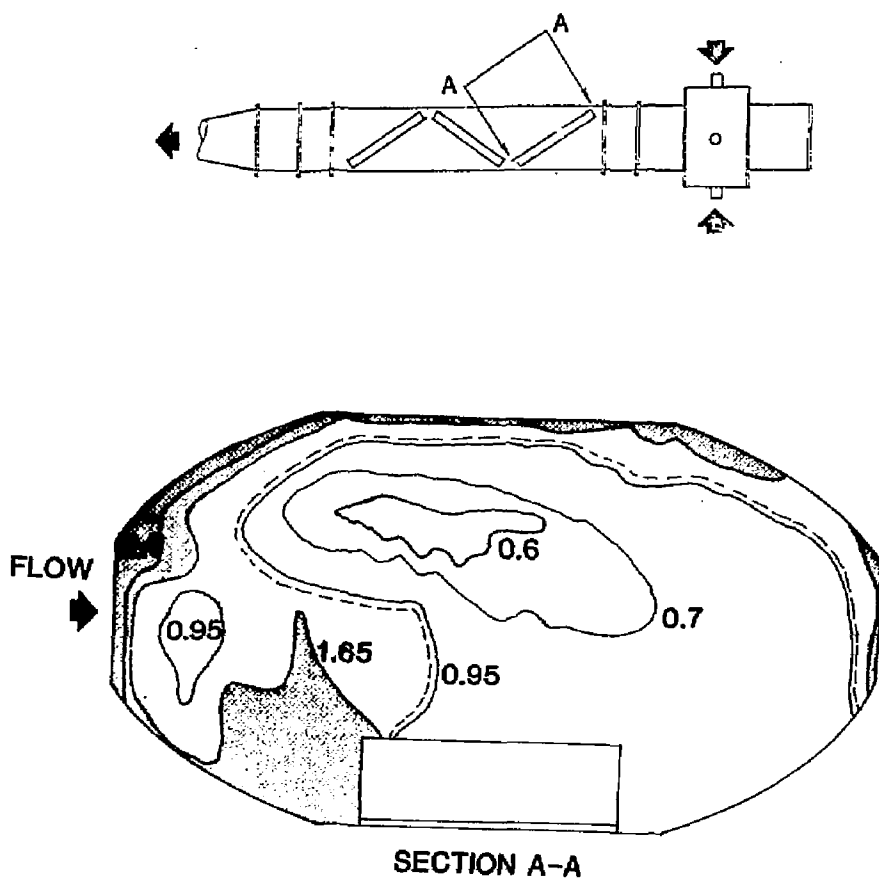


Figure B.3. Case I - No Inner Liner: Distribution of h^* on Back Surface of First Laser Disk.

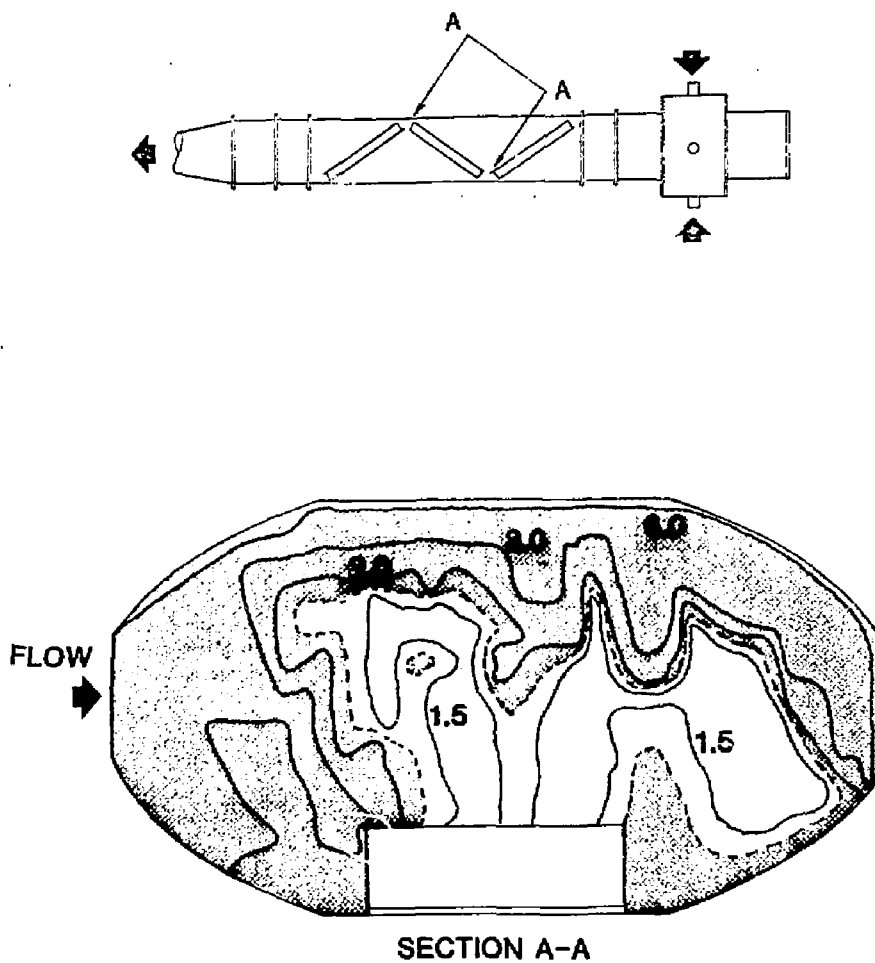


Figure B.4. Case I - No Inner Liner: Distribution of h^* on Front Surface of Second Laser Disk.

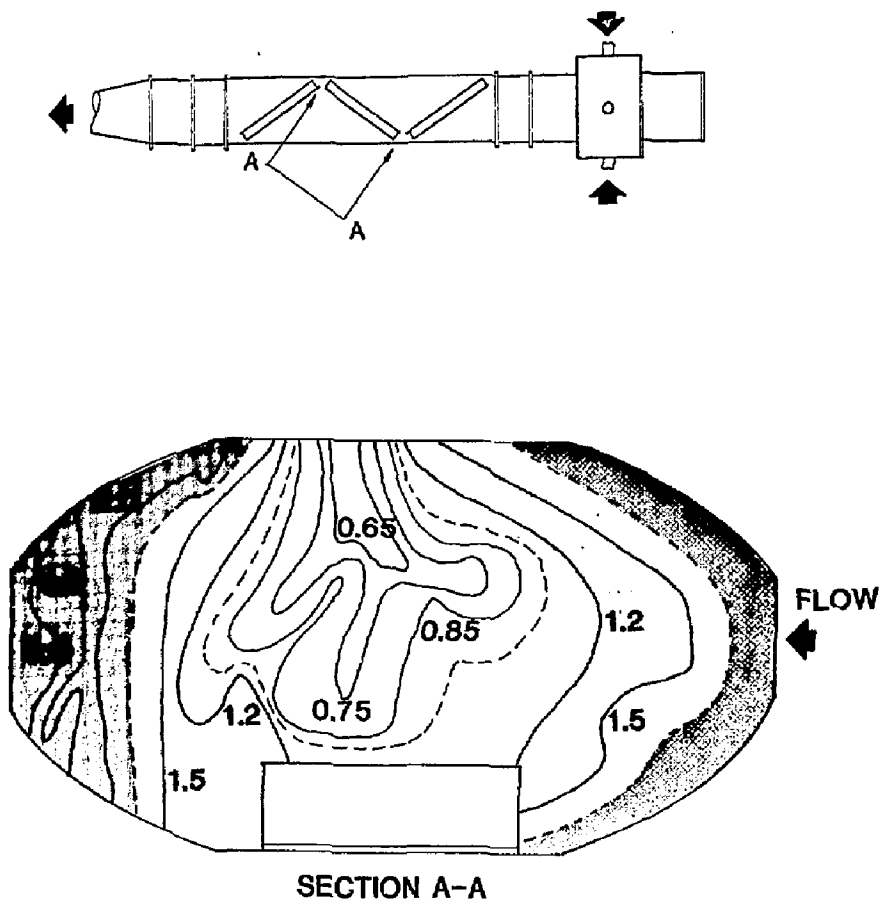


Figure B.5. Case I - No Inner Liner: Distribution of h^* on Back Surface of Second Laser Disk.

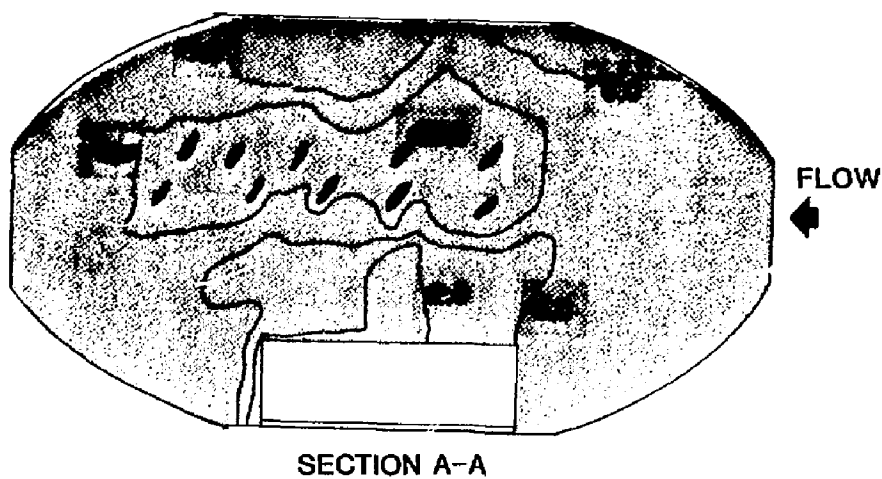
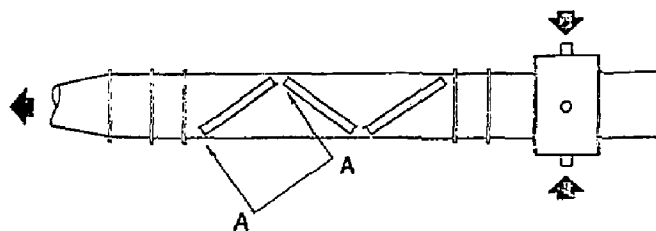


Figure 8.6. Case I - No Inner Liner: Distribution of h^* on Front Surface of Third Laser Disk.

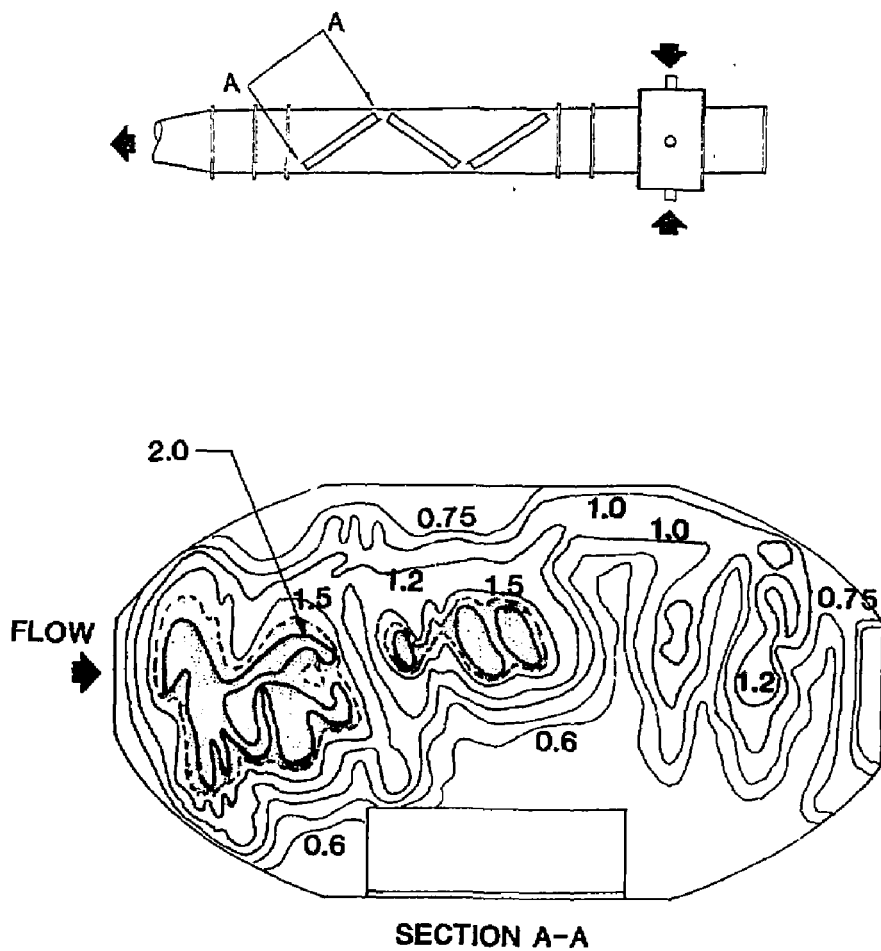


Figure B.7. Case I - No Inner Liner; Distribution of h^* on Back Surface of Third Laser Disk.

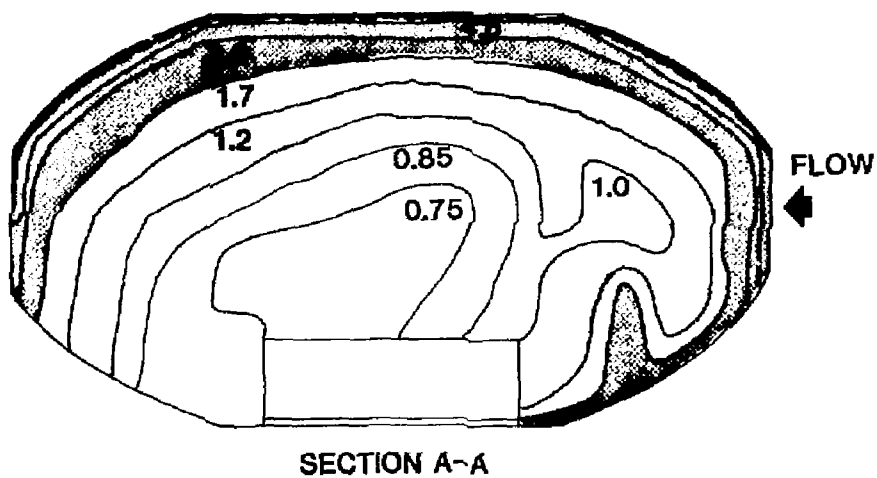
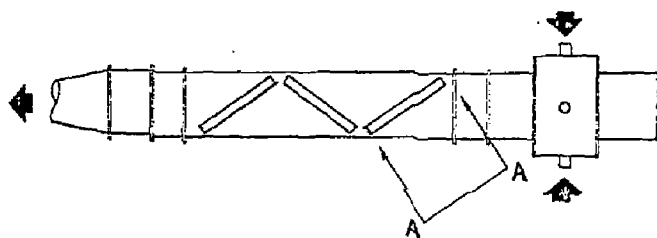


Figure B.8. Case 11 - Plenum with Vanes at 0° : Distribution of h^* on Front Surface of First Laser Disk.

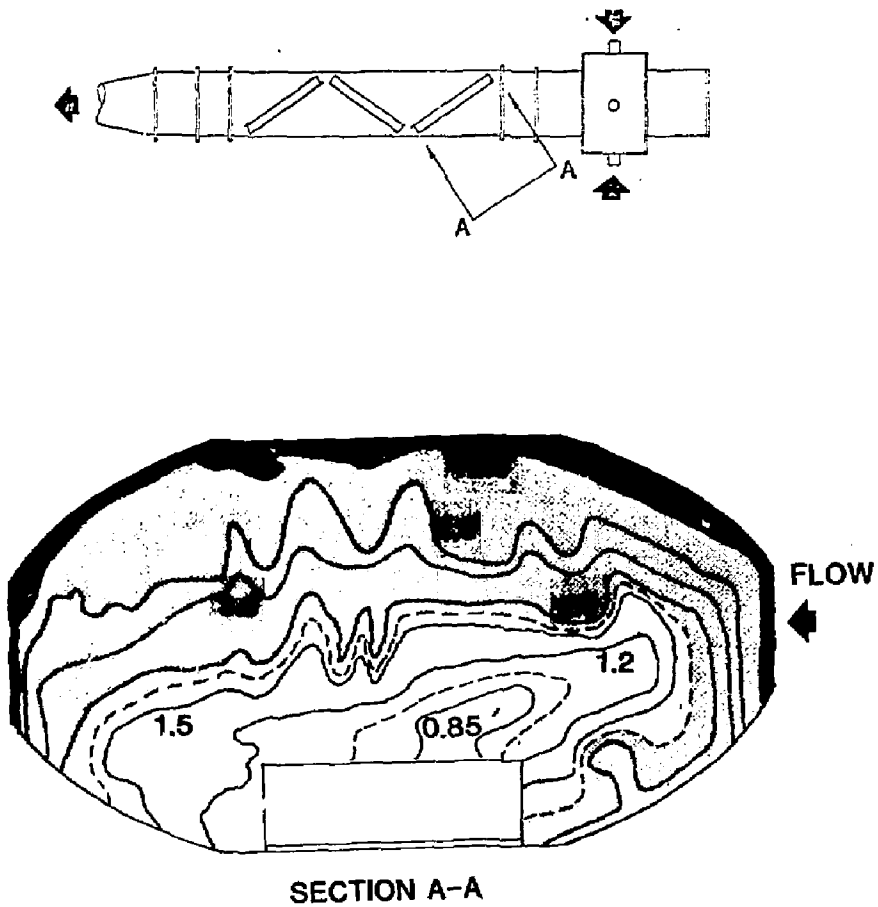


Figure B.9. Case III - Plenum with Vanes at 45° : Distribution of h^* on Front Surface of First Laser Disk.

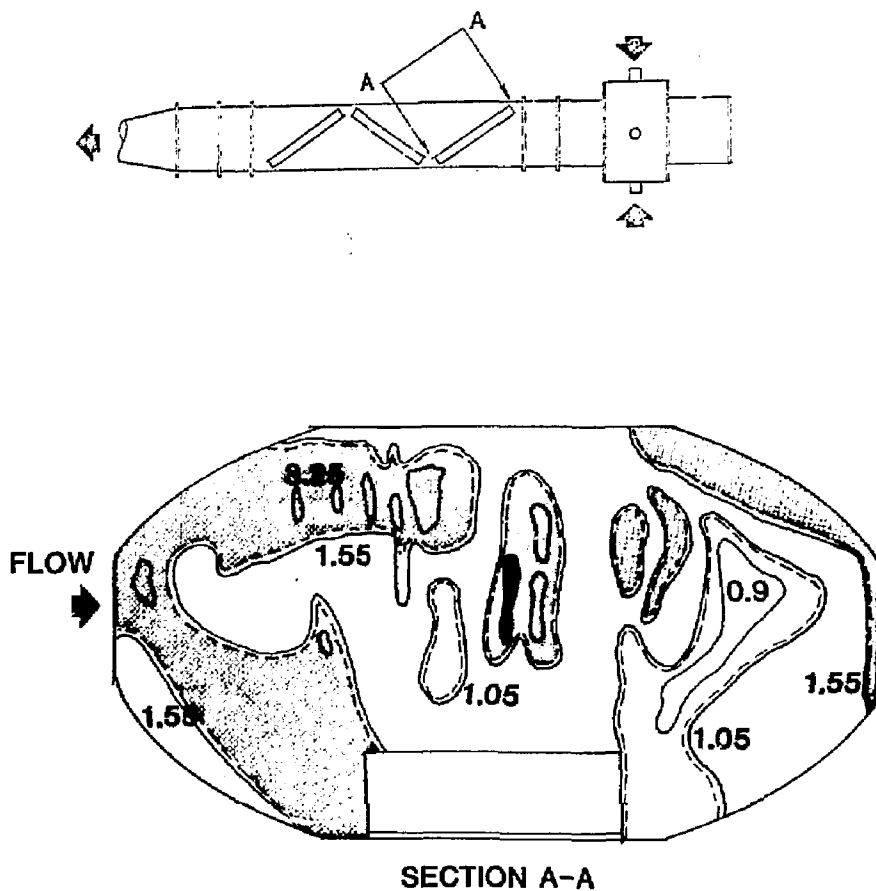


Figure B.10. Case III - Plenum with Vanes at 45° : Distribution of h^* on Back Surface of First Laser Disk.